Title:

Transport of trace metals (Mn, Fe, Ni, Zn and Cd) in the western Arctic Ocean (Chukchi Sea and Canada Basin) in late summer 2012

Authors:

Y. Kondo[1, 2*], H. Obata[3], N. Hioki[4], A. Ooki[4], S. Nishino[5], T. Kikuchi[5], K. Kuma[4]

Institutional addresses:

[1] Arctic Environment Research Center, National Institute of Polar Research, Japan

[2] Graduate School of Fisheries and Environmental Sciences, Nagasaki University, Japan

[3] Atmosphere and Ocean Research Institute, The University of Tokyo, Japan

[4] Faculty of Fisheries Sciences, Hokkaido University, Japan

[5] Institute of Arctic Climate and Environment Research, Japan Agency for Marine-Earth Science and Technology, Japan

Corresponding author's email: yoshikondo@nagasaki-u.ac.jp

Abstract

Distributions of trace metals (Mn, Fe, Ni, Zn and Cd) in the western Arctic Ocean (Chukchi Sea and Canada Basin) in September 2012 were investigated to elucidate the mechanisms behind the transport of these metals from the Chukchi Shelf to the Canada Basin. Filtered (< 0.22 μm) and unfiltered seawater samples were analyzed to determine dissolved (D) and total dissolvable (TD) trace metal concentrations, respectively. We identified maxima in vertical profiles for the concentrations of D-Fe and TD-Fe, as well as for the other four analyzed trace metals, which occurred in the halocline and/or near-bottom waters. Concentration profiles of all trace metals except for Cd also tended to show peaks near the surface, which suggest that the inflow of low-salinity Pacific-origin water from the Bering Strait, as well as local fresh water inputs such as river water and melting sea-ice, influenced trace metal concentrations. The distribution patterns and concentration ranges were generally similar between the D and TD fractions for Ni, Zn and Cd, which indicate that Ni, Zn and Cd were present mainly in their dissolved forms, whereas the concentrations of TD-Fe and TD-Mn were generally higher than those of D-Fe and D-Mn, respectively. These results are consistent with the results of previous studies of this region. For both Fe and Mn, labile particulate (LP) concentrations (the difference between the TD and D fractions, which is acid-leachable fraction in the particles during storage at pH 1.5-1.6) were highest in the near-bottom waters of the Chukchi Shelf region. The relationships between the distance from the shelf break and the concentrations of trace metals revealed that Fe and Mn concentrations in halocline waters tended to decrease logarithmically with distance, whereas changes in the concentrations of Ni, Zn, Cd and phosphate with distance were small. These results suggest that the distributions of Fe and Mn were controlled mainly by input from shelf sediment and removal through scavenging processes. Based on the phase distributions of Fe and Mn, which were calculated as ratios between the LP and D fractions, different behaviors between Fe and Mn were expressed during lateral transportation. The concentration of TD-Fe declined

rapidly via removal of LP-Fe from the water column, whereas the concentration of TD-Mn declined more slowly through the transformation of D-Mn into LP-Mn. In contrast, the concentrations of D-Cd, D-Zn and D-Ni were more strongly correlated with phosphate levels, which suggest that, like phosphate, the distributions of Cd, Zn and Ni were generally controlled by the internal biogeochemical cycles of the ocean interior. Based on the findings of studies that have previously evaluated the concentration maxima of Ni, Zn and Cd within the halocline layer in the Canada Basin near the Canadian Arctic Archipelago, the elevated Ni, Zn and Cd concentrations in the halocline layer may extend across the Canada Basin from the Chukchi Sea shelf-break area. The determination coefficients for correlations with phosphate concentration varied between the concentrations of Ni, Zn and Cd, which suggest that the sources of these trace metals, such as sediments and sea-ice melting, affected their patterns of distributions differently. Our findings reveal the importance and impact of the halocline layer for the transport of trace metals in the western Arctic Ocean during the late summer. The existence of rich and various sources likely sustained the high concentrations of trace metals and their unique profiles in this region.

Key words: Trace metals, Arctic Ocean, Chukchi Sea, Canada Basin, halocline, GRENE

1. Introduction

Although the Arctic Ocean constitutes only about 3% of the world's oceans by area, it includes approximately 20% of the world's continental shelf area (Chang and Devol, 2009). The Chukchi Sea, located in the western Arctic Ocean, is a highly productive region during times of ice-edge retreat (Hill and Cota, 2005). Physical, chemical and biological characteristics of the Chukchi Sea are strongly influenced by currents that flow northward through the Bering Strait (Springer and McRoy, 1993). The mean annual transport through the Bering Strait into the Chukchi Sea is about 0.8 Sv, which has strong seasonal variability between a summer maximum and a winter minimum, and supports the high productivity of this region through the transport of nutrients (Coachman and Aagaard, 1988). It has been reported that a large fraction of the organic matter that forms in surface waters in the shelf areas of the Chukchi Sea sinks to the seafloor, which fuels productive benthic communities and causes high rates of sedimentary denitrification (Chang and Devol, 2009; Brown *et al.*, 2015). The Pacific-origin water from the Bering Strait is already depleted in nitrate (NO_3^-) relative to phosphate (PO_4^{3-}), and NO_3^- is further depleted relative to PO_4^{3-} in the Chukchi Sea via the effect of sedimentary denitrification (Yamamoto-Kawai *et al.*, 2006). A unique feature of the upper surface water in the western Arctic Ocean is the dominance of a strong, cold halocline that separates the Pacific-origin surface waters from the underlying Atlantic-origin waters (Aagaard *et al.*, 1981). Cold and dense brine is produced in the fall and winter as sea ice forms, and the halocline is maintained by large-scale lateral advection from the adjoining continental shelves (Aagaard *et al*., 1981; Jones and Anderson, 1986). The water of this halocline is therefore associated with prominent maxima of nutrients and dissolved organic matter (Anderson *et al.*, 2013). In the Canada Basin, mixtures of Pacific-origin and Atlantic-origin waters are only found below the nutrient maxima (Yamamoto-Kawai *et al.*, 2008). Pacific-origin water that enters through the Bering Strait can be highly modified throughout transport on the shelves by runoff, interaction between sediment and near-bottom

water, and sea-ice formation (Cooper *et al.*, 1997). The Canada Basin is separated from the Makarov Basin by the Mendeleev–Alpha Ridge with a sill depth of ~2000 m, and is fairly isolated from ventilation by the dense shelf waters of the Makarov, Barents, Kara and Laptev seas (Swift *et al.*, 1997). In the Canada Basin, freshening of surface seawater began in the 1990s and has been attributed to increased river runoff and sea ice melting (Morison et al. (2012) and references therein).

Trace metals such as iron (Fe), manganese (Mn), nickel (Ni), zinc (Zn) and cadmium (Cd) are involved in numerous processes in the metabolisms of phytoplankton and can be toxic at high concentration (Twining and Baines, 2013 and references therein). Iron is required for many processes including photosynthesis, chlorophyll synthesis and nitrogen metabolic pathways such as nitrogen fixation and NO_3^- and nitrite (NO_2^-) reduction. It is well established that Fe often limits phytoplankton growth in environments where subsurface nutrients are replete, which include high-nutrient, low-chlorophyll areas such as the upwelling regions of the Southern Ocean and the eastern equatorial Pacific (e.g., Moore *et al.*, 2013). Zinc also plays a role in many metalloproteins such as alkaline phosphatase, carbonic anhydrase and the Zn form of superoxide dismutase (Zn-SOD). Cadmium is also known to be a cofactor in carbonic anhydrase, and can substitute for Zn in diatom growth pathways (Lane and Morel, 2000); it has been suggested that phytoplankton mistakenly import Cd through a non-specific divalent metal transporter in this process (Horner *et al.*, 2013). Sunda and Huntsman (2000) demonstrated that Cd drawdown was accelerated under Fe-limited conditions. Nickel is associated primarily with urease and the Ni form of superoxide dismutase (Ni-SOD) (Dupont *et al.*, 2008a, b). Manganese is an essential trace metal for phytoplankton growth because it is prominently involved in the oxygen-evolving complex of photosystem II and the Mn form of superoxide dismutase (Mn-SOD) (Wolfe-Simon *et al.*, 2005). However, limitation of Mn for phytoplankton growth has not yet been observed in the ocean.

In the open ocean, vertical distributions of Ni, Zn and Cd in dissolved fractions (< 0.2–0.4 μ m) are generally characterized by surface minima, rapid increases to maximum concentrations in the thermocline, and then relatively constant concentrations in deep water, similar to the distribution patterns of nutrients (e.g., Bruland *et al.*, 1991). However, the vertical distributions of dissolved Mn and Fe differ from those of the above "nutrient-type" trace metals. Maximum Mn occurs in the surface water and decreases with depth, which is why Mn is called a "scavenging-type" trace metal (e.g., Bruland *et al*., 1991). Vertical profiles of Fe are often reported as nutrient-type or a combination of nutrient-type and scavenging-type elements; therefore, Fe is called as "hybrid-type" trace metal. Both Fe and Mn have short residence times relative to Ni, Zn and Cd (Chester and Jickells, 2012). In oxygenated seawater, the thermodynamically favored form of Fe is Fe(III), which is strongly hydrolyzed, and its removal is mainly constrained by complexation with natural organic ligands such as humic substances (Laglera *et al.*, 2011).

Recent studies have gradually revealed the distribution of Fe in the western Arctic Ocean (Chukchi Sea and Canada Basin). The reported ranges for the concentrations of dissolved Fe and total dissolvable Fe (i.e., the concentration of leachable Fe in acidified unfiltered sample, see section 2) have been extremely broad (0.36–33.1 nM and 0.8–89000 nM, respectively), but the maxima of dissolved Fe concentration occurred consistently within the halocline layer (HL) with high concentrations of nutrients and dissolved organic matter (Nakayama *et al.*, 2011; Cid *et al.*, 2012 ; Nishimura *et al.*, 2012; Aguilar-Islas *et al.*, 2013; Hioki *et al.*, 2014). Because high concentrations of trace metals have been observed in near-bottom water in the shelf region, it has been suggested that sedimentary input is an important source of trace metals in the western Arctic Ocean. However, few studies of trace metals (especially Mn and Fe) in Chukchi Sea sediments have been performed (Naidu *et al.*, 1997; Trefry *et al.*, 2014). Naidu *et al*. (1997) investigated metal concentrations (Al, Fe, Mn, Cu, Cr, Co, Zn, Ni and V) in the seafloor muds of the Chukchi Sea in 1986, and found that the

concentrations of these metals were low relative to those of Arctic shelves of Russia, East Greenland and the Beaufort Sea. A more recent study also investigated concentrations of Fe, Al and selected trace metals (including Mn, Cd, Ni, Zn) in surface sediments from the Chukchi Sea collected in 2009 and 2010; although concentrations of each trace metal varied considerably with sediment texture (i.e., grain size), these metals were found to exist at natural background levels in most samples when normalized for Al concentration (Trefly *et al*., 2014). These studies suggest that Chukchi Shelf sediment is unlikely to have been significantly influenced by anthropogenic pollution. In addition to continental shelf sediments and remineralization of biogenic and/or mineral particles, river discharge and melting sea ice are also potential sources of trace metals (Nakayama *et al*., 2011; Nishimura *et al*., 2012; Cid *et al*., 2012; Hioki *et al*., 2014). The presence of these diverse sources is likely to influence the lateral transport of Fe in this region. Compared to Fe, there are relatively few data for distributions of Zn, Cd, Ni and Mn in the western Arctic Ocean (Yeats, 1988; Yeats and Westerlund, 1991; Cid *et al*., 2012). Yeats (1988) and Yeats and Westerlund (1991) investigated the distributions of total dissolvable Mn, Co, Ni, Cu, Zn and Cd and dissolved Mn in the Canada Basin near the Canadian Arctic Archipelago, and found that Ni, Zn and Cd concentrations tended to peak around the nutrient maximum in the halocline. More recently, Cid *et al*. (2012) investigated distributions of trace metals (Al, Mn, Fe, Co, Ni, Cu, Zn, Cd and Pb) from samples collected in September 2000 and found that roughly all of these trace metals had concentration maxima in the HL, with the exception of Al. It was suggested that nutrient-type trace metals such as Ni, Cu, Zn and Cd were generally more dominant in the dissolved fractions (< 0.2 μm), whereas the other metals measured (Al, Mn, Fe and Co) were more dominant in the labile particulate fractions (i.e., the differences between dissolved and total dissolvable fractions) (Cid *et al*., 2012). However, the mechanism behind the transport of these trace metals from the Chukchi Shelf to the Canada Basin remains unclear.

The balance between input and removal of a trace metal controls its distribution in seawater. As discussed above, there are several potential sources of trace metals in the western Arctic Ocean, and the processes associated with each source and sink are likely to have different impacts on the concentrations of different trace metals that reflect their specific characteristics. Therefore, it is valuable to investigate the distributions of many trace metals simultaneously to elucidate geochemical cycling in this region. Furthermore, the climatic conditions of the Arctic Ocean have changed rapidly over the previous several decades, which have resulted in environmental impacts such as decreased summer sea-ice cover and increased air temperature (Wood *et al.*, 2015). Indeed, in the summer of 2012, the area of the Arctic Ocean covered by sea ice was the smallest in recorded history (National Snow and Ice Data Center (NSIDC) (http://nsidc.org/data/seaice_index/)). For this study, the distributions of dissolved and total dissolvable trace metals (Mn, Fe, Ni, Zn and Cd) in the Chukchi Sea and Canada Basin were investigated to elucidate the transport of trace metals in the western Arctic Ocean in the late summer of 2012.

2. Methods

2.1. Study area and sample collection

Seawater samples were collected from the western Arctic Ocean during the R/V *Mirai* (Japan Agency for Marine Earth Science and Technology – JAMSTEC) MR12-E03 cruise from September 15 to October 4, 2012 (Kikuchi, 2012; Fig. 1). The samples were obtained using acid-cleaned, Teflon-coated 10-L Niskin-X sampling bottles with a Teflon sampling spigot (General Oceanics) attached to a Conductivity Temperature Depth–Carousel Multiple Sampler (CTD-CMS, SBE 911 Plus and SBE 32 carousel water sampler, Sea-Bird Electronics, Inc.) and armored cable. All plastic apparatus used for this study were acid-cleaned. Filtered (< 0.22 μm, Durapore cartridge Millipak 100, Millipore) and unfiltered seawater samples were collected to determine the concentrations of dissolved trace metals

(D-metals: D-Mn, D-Fe, D-Ni, D-Zn and D-Cd) and total dissolvable trace metals (TD-metals: TD-Mn, TD-Fe, TD-Ni, TD-Zn and TD-Cd), respectively. Gravity filtration was performed for the filtered samples in a hangar deck of the ship immediately after recovering the Niskin-X sampling bottles. Since the seawater samples used for this study were obtained from the same Niskin-X sampling bottles at the same time as those used for previous Fe analyses (Hioki *et al*., 2014), the seawater samples were identical between two studies. All samples were collected in 125-mL low-density polyethylene (LDPE, Nalgene) bottles and acidified to pH 1.5-1.6 with 0.5-mL trace-metal-grade HCl (Tamapure AA100, Tama Chemical) in a class 100 clean air bench on board the research vessel. The acidified samples were stored at room temperature for over two years before the trace metals analyses were performed in a land-based laboratory.

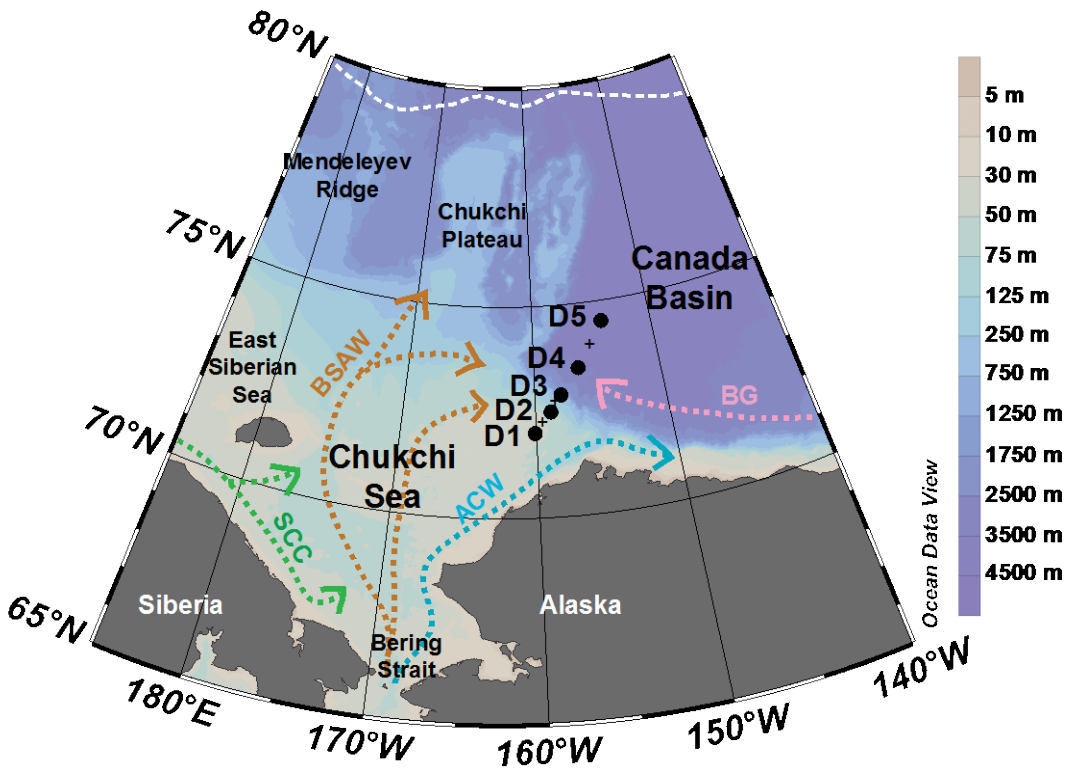

Fig. 1. Sampling locations (black filled circles) during R/V *Mirai* MR12-E03 cruise. Cross symbols indicate the locations that only hydrographic parameters and nutrients data were obtained. White dot-line indicates the location of ice edge during the observation. Dot-arrows indicate the surface water currents directions in this region (pink: Beaufort Gyre

(BG), sand: Bering Shelf Anadyr Water (BSAW), cyan: Alaskan Coastal Water (ACW), green: Siberian Coastal Current (SCC)).

2.2. Trace metal analyses

The concentrations of D-metals ([D-Mn], [D-Fe], [D-Ni], [D-Zn] and [D-Cd]) and TD-metals ([TD-Mn], [TD-Fe], [TD-Ni], [TD-Zn] and [TD-Cd]) were determined using a chelating resin preconcentration and inductively coupled plasma mass spectrometry (ICP-MS) method adapted from Sohrin *et al*. (2008). Preparation of all reagents and samples was carried out in a positive-pressure class 1000 clean room. All apparatus used for sample preparation were acid-cleaned before use. For preconcentration of each sample, Nobias Chelate-PA1 (Hitachi High-Technologies) resin was packed in a column of a 3-cm perfluoroalkoxy alkane tube with a 1.8-cm in diameter. Acetic acid - ammonium acetate buffer (pH of 6.0) was prepared by mixing trace-metal-grade NH_4OH (Tamapure AA100, Tama Chemical) and glacial acetic acid (Optima, Fisher Chemical), where final concentration of acetic acid plus acetate was 3.6 M. A 0.05 M acetate buffer was prepared by diluting the 3.6 M buffer solution. The Nobias Chelate-PA1 column was mounted in a manual preconcentration system. Fig. 2 illustrates the procedure for the sample preconcentration and extraction steps. Prior to the sample being loaded, the chelating resin column was cleaned using >35 mL of 2 M HNO_3 (trace-metal-grade, Tamapure AA100, Tama Chemical) and conditioned using 35 mL of 0.05 M acetate buffer solution. Then each seawater sample (24.5 mL) was delivered into the column with a peristaltic pump. After the seawater sample was loaded, 17.5 mL of 0.05 M ammonium acetate buffer solution was passed through the column to remove sea salt in the column. The trace metals were then eluted with 6 mL of 2 M HNO_3. The system used for this study had four parallel lines and could process four samples simultaneously. The flow rate was 3.5 mL/min for the sample, buffer solutions and acid for the cleaning column; the flow rate for the eluent (6 mL of 2 M HNO_3) was 1.5 mL/min using

a Teflon syringe opposite the direction of sample loading. Consequently, each seawater sample was concentrated 4.1 times into 2 M HNO_3. Concentrations of D-metals or TD-metals in the eluent were determined with a Thermo Scientific ELEMENT XR mass spectrometer using the medium resolution mode in a clean room; a calibration curve method was applied using a diluted metal standard solution (ICP-MS Multi-Element Solution, SPEX) prepared in 2 M HNO_3. The isotopes measured for the determinations were ^{55}Mn, ^{57}Fe, ^{60}Ni, ^{68}Zn and ^{114}Cd. Other isotopes for Fe (^{56}Fe), Ni (^{61}Ni and ^{62}Ni), Zn (^{66}Zn and ^{67}Zn) and Cd (^{111}Cd and ^{112}Cd) were also measured to cross-check the results. For this study, the detection limits, defined as three times the standard deviation of the blank seawater measurements (n = 4–8), were 0.012 nM, 0.25 nM, 0.091 nM, 0.19 nM and 0.095 nM for Mn, Fe, Ni, Zn and Cd, respectively. The standard seawater samples GEOTRACES GD and SAFe D2 (Johnson *et al*., 2007) were run as quality control checks for the data (Table 1), and the results were within or near the ranges of the most recent consensus values (GEOTRACES website (2015): http://www.geotraces.org/science/intercalibration).

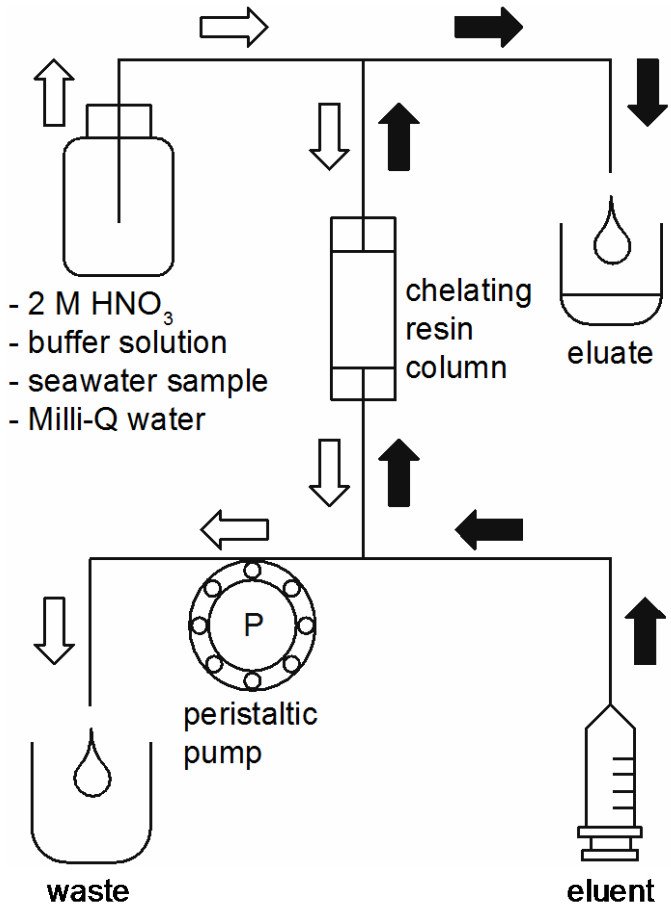

Fig. 2. Diagram of the preconcentration system of trace metals. White arrows mean the flow direction when seawater sample is introduced to the chelating resin column. Black arrows mean the one when eluent pass through the column.

2.3. Hydrographic data

Temperature and salinity were measured with a CTD probe. Data for chlorophyll *a* and dissolved oxygen concentrations were obtained with a chlorophyll fluorometer and an oxygen sensor, respectively. The concentrations of nutrients (indicated with square brackets: [NO_3^-], [NO_2^-], [NH_4^+], [PO_4^{3-}] and [$Si(OH)_4$]) were measured with a QuAAtro system by Marine Works Japan. Details of these analytical methods are provided in the cruise report for the R/V *Mirai* cruise MR12-E03 (Kikuchi, 2012). The report and data are available to the public through the JAMSTEC data website (http://www.godac.jamstec.go.jp/darwin/e).

3. Results

3.1. Hydrography

Fig. 3 is a temperature–salinity diagram that shows the existence of several water masses in the study area, which is consistent with the findings of previous studies (Shimada *et al*., 2005; Codispoti *et al*., 2005; Wang *et al*., 2006; Cid *et al*., 2012; Aguilar-Islas *et al*., 2013; Hioki *et al*., 2014). We divided these masses into four types based on salinity and potential density (σ_θ): (1) Pacific Summer Water (PSW), which extends from the surface to depths of ~ 10–75 m, and has salinity ≤ 32.0 and $\sigma_\theta \leq 25.6$; (2) the Upper Halocline Layer (UHL), which has salinity of 32.0–33.6 and σ_θ of 25.7–27.0; (3) the Lower Halocline Layer (LHL) with salinity of 33.6–34.5 and σ_θ of 27.1–27.7; and (4) Atlantic Water (AW) with salinity ≥ 34.6 and $\sigma_\theta \geq 27.8$. In this study, the UHL and LHL together are defined as HL. Note that the near-bottom waters at Stns. D1 and D2 were within the UHL in this study.

Distributions of potential temperature, salinity, σ_θ, dissolved oxygen and nutrients are shown in Fig. 4. The surface area of sea ice covering the Arctic Ocean reached its lowest recorded extent in the summer of 2012 (National Snow and Ice Data Center (NSIDC) (http://nsidc.org/data/seaice_index/)) when our observations and sample collection were performed. Our sampling site was over 500 km from the nearest ice edge. However, sea ice persisted until September around Wrangel Island between the Chukchi Sea and East Siberian Sea in 2012, Nishino et al. (2016) found the large fraction of sea-ice meltwater relative to a more typical year in the Chukchi Sea using a calculated fraction of sea-ice meltwater (f_{SIM}) from the relationship between potential alkalinity (total alkalinity + nitrate – ammonium) and salinity (Yamamoto-Kawai *et al.*, 2009). In this study, salinity in the surface water (5-m depth) was generally low (25.1–28.2); the lowest value was observed from the offshore station (Stn. D5). Although inflows of meteoric fresh water and low-salinity Pacific-origin water through the Bering Strait are likely to influence the distribution of salinity in this study area (e.g., Shimada *et al*., 2005; Yamamoto-Kawai *et al*., 2008), the f_{SIM} in the surface water

at Stn. D5 was higher (f_{SIM} = 0.06) than those at adjacent stations (f_{SIM} = 0.02–0.05) except for Stn. D1 (f_{SIM} = 0.08), suggesting that the surface water at Stn. D5 was relatively influenced by sea-ice melting (Japan Agency for Marine-Earth and Technology (2016) Data Research System for Whole Cruise information in JAMSTEC). These things indicate the presence of freshwater input from rivers and melting sea-ice via Ekman transport associated with the Beaufort Gyre (Proshutinsky *et al*., 2009).

The cold halocline water forms a barrier to mixing of the Pacific-origin surface waters and underlying Atlantic waters. All nutrients analyzed had maxima in the UHL, although the patterns of their vertical profiles were variable among them. In the PSW, dissolved inorganic nitrogen (DIN, sum of NO_3^-, NO_2^- and NH_4^+) was largely depleted relative to PO_4^{3-} at all stations, which suggests that phytoplankton growth may be limited by nitrogen in this area; this finding is consistent with previous studies of this region (Codispoti *et al*., 2005; Wang *et al*., 2006; Brown *et al*., 2015). Indeed, chlorophyll *a* concentration never exceeded 0.5 μg/L at all stations; its maximum was observed at 10–20-m depths at Stns. D1, D2 and D3, 50-m depth at Stn. D4 and 100-m depth at Stn. D5 (Table 2). Because a subsurface chlorophyll maximum exceeding 1 μg/L was found over the Chukchi Shelf region in August (Hill *et al*., 2005; Wang *et al*., 2006), a decline in phytoplankton blooming during our observational period can be presumed. Below the PSW, [NO_3^-] increased to as high as 16 μM in the UHL, and then decreased to ~ 13 μM in the AW. Contour plots of [NO_2^-] and [NH_4^+] in 2D sections revealed that these nutrients had clear maxima in the UHL near the shelf and slope regions of the Chukchi Sea. In particular, [NH_4^+] frequently accumulated (> 1 μM) in the UHL, as reported in previous studies (Codispoti *et al*., 2005; Connelly *et al*., 2014; Brown *et al*., 2015). Brown *et al*. (2015) investigated the stable isotopes of oxygen (^{16}O and ^{18}O) and nitrogen (^{14}N and ^{15}N) of NO_3^-, which suggested that the main source of the accumulated NH_4^+ near the bottom water in the Chukchi Sea shelf region was sedimentary input, not the degradation of organic matter in the water column. In contrast with DIN, both PO_4^{3-} and

$Si(OH)_4$ were replete in the study area. There were clear maxima in the UHL for both [PO_4^{3-}] and [$Si(OH)_4$], and the highest values were observed in the UHL at Stn. D3 where dissolved oxygen concentration was low. Interestingly, [$Si(OH)_4$] in the PSW at Stns. D4 and D5 were lower than those at Stns. D1, D2 and D3, whereas other nutrients, such as PO_4^{3-}, did not show this trend. Tovar-Sánchez *et al*. (2010) reported that concentrations of total phosphorus and nitrogen in Arctic sea ice were ~ 24% and ~ 70% of those in surface seawater, respectively, whereas the concentrations of $Si(OH)_4$ were only ~ 5% of those in the surface water. These results also reflect the influence of sea-ice melting at the Canada Basin stations (Stns. D4 and D5) during our observations.

Fig. 4 also shows the 2D section of N^*, which is a commonly used metric to assess the degree of deficiency or excess of nitrogen in a water mass relative to phosphorus, originally defined as $N^* = ([NO_3^-] - 16[PO_4^{3-}] + 2.9) \times 0.87$ (Gruber and Sarmiento, 1997). Because DIN includes NO_2^- and NH_4^+ in addition to NO_3^-, we adopt a definition where $N^* = ([DIN] - 16[PO_4^{3-}] + 2.9) \times 0.87$ for the western Arctic Ocean (Nishino *et al.*, 2005). A negative N^* indicates DIN loss or PO_4^{3-} input for a region, whereas a positive N^* indicates DIN input or PO_4^{3-} loss. Consequently, a water mass with a high N^* value generally has high nitrogen input through nitrogen fixation, and one with a low N^* value is generally nitrogen deficient from sedimentary and/or water column denitrification. In the study area, N^* was negative in the PSW and HL (Hioki *et al*., 2014), which is consistent with the findings of previous studies of the Chukchi Sea (e.g., Nishino *et al.*, 2005; Connelly *et al*., 2014); in fact, the Chukchi Shelf is considered to be have some of the lowest N^* values globally (Deutsch and Weber, 2012). N^* in the UHL was lower than in other water masses, and the lowest N^* was observed near the bottom at the shelf break station (Stn. D2). Because dissolved oxygen concentrations in the study area were too high to enable denitrification in the water column, the low N^* suggests that the water mass was influenced by sedimentary denitrification and/or

anammox. In contrast, however, *N** in the AW was found to show positive values, which reflects the difference between Pacific- and Atlantic-origin waters in this area.

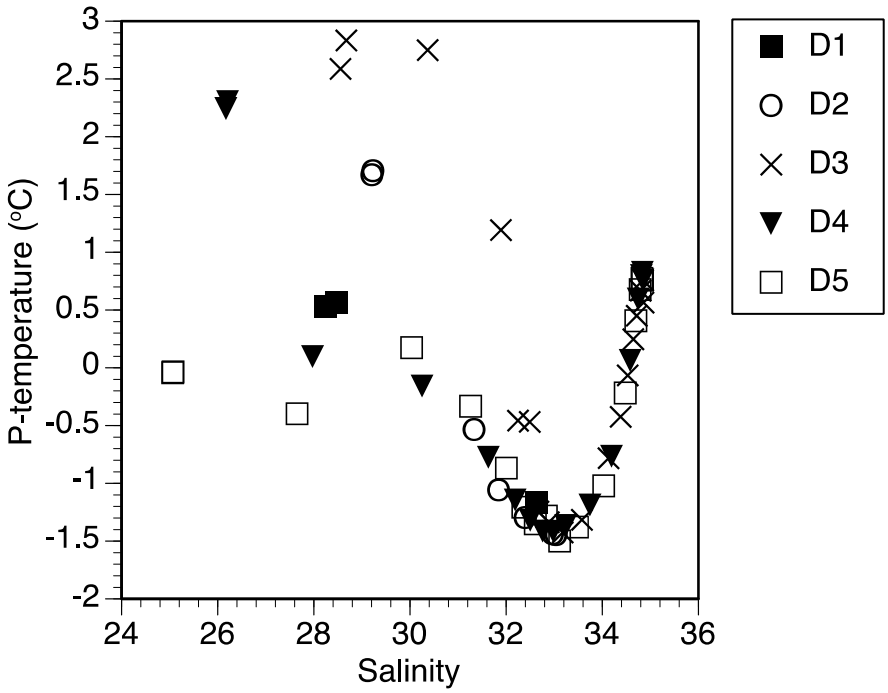

Fig. 3. Temperature - salinity diagram from the sampling sites in this study.

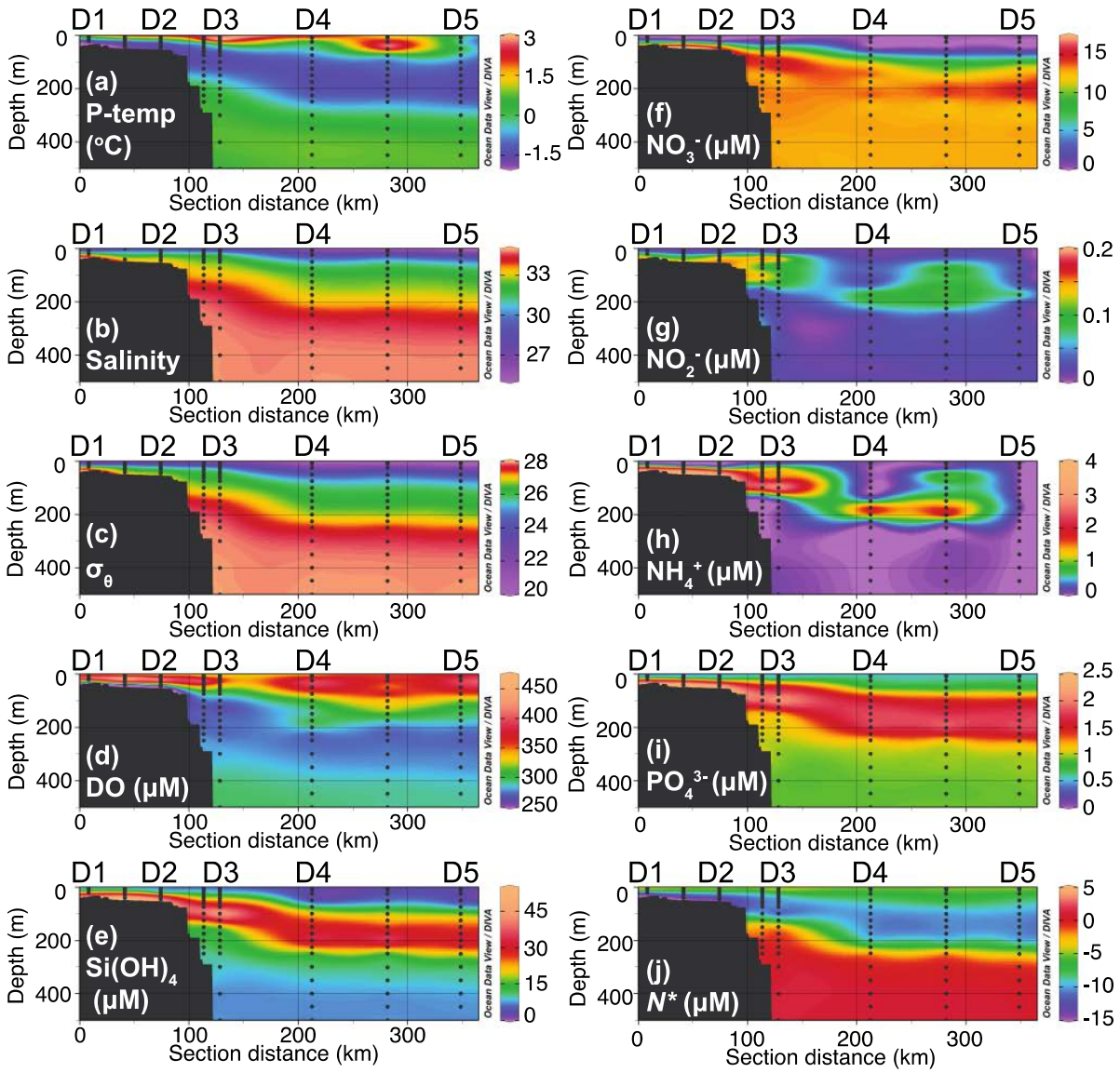

Fig. 4. Upper 500 m vertical sections from Stns. D1 to D5 for (a) potential temperature (P-temp), (b) salinity, (c) potential density (σ_θ), (d) dissolved oxygen (DO), (e) $Si(OH)_4$, (f) NO_3^-, (g) NO_2^-, (h) NH_4^+, (i) PO_4^{3-} and (j) N^*. N^* was calculated from the following equation; $N^* = ([DIN] - 16[PO_4^{3-}] + 2.9) \times 0.87$ (see text).

3.2. Dissolved trace metals (D-metals) in the Chukchi Sea and Canada Basin

The spatial distributions of D-metals are shown in Figs. 5 and 6, and the corresponding datasets are given in Table 2. The [D-Fe] ranged from 0.78 to 8.26 nM. In the PSW, [D-Fe] was high, with an average of 1.52 ± 0.42 nM (n = 13) including the samples from the Canada Basin (Stn. D4). The [D-Fe] reached its peak in the surface water (5-m depth) at all stations

except for Stn. D5, where [D-Fe] could not be determined because of contamination; the highest surface [D-Fe], 2.65 nM, was found at the Chukchi Sea shelf slope (Stn. D3). Below the surface, [D-Fe] decreased to minima near the subsurface chlorophyll maximum layers at Stns. D1, D2 and D3, which suggest Fe consumption by phytoplankton (Table 2). Then, [D-Fe] began to increase with depth in the UHL, and an especially high [D-Fe] of over 6 nM was found only near the bottom in the Chukchi Sea. The highest [D-Fe] was observed near the bottom in the vicinity of the Chukchi Sea shelf break (Stn. D2). It was also recognized based on the relationship between [D-Fe] and salinity that the highest [D-Fe] was observed around salinity of ~ 33.6, which occurred at the boundary between the UHL and LHL (Fig. 7). This trend was also observed in the relationships between nutrients such as [PO_4^{3-}] and salinity (Fig. 7), although the relationship between [D-Fe] and salinity was more complex. Within the UHL, [D-Fe] gradually decreased with distance from the shelf (see section 4.3); the peak of [D-Fe] in the UHL was no longer apparent at Stn. D5 (Fig. 6). In the AW, the [D-Fe] ranged from 0.78 to 2.34 nM, and there was no clear trend in the distribution patterns between stations.

The [D-Mn] covered a broad range from 0.34 to 81.4 nM (Figs. 5, 6 and Table 2), which fall within the range determined in a previous study of the western Arctic (Cid *et al*., 2012). Except for Stn. D1, the vertical distribution of [D-Mn] had 2 peaks: one in the surface water and a second in the UHL. In the surface water (5-m depth), the [D-Mn] ranged from 8.21 to 15.0 nM with a mean of 10.81 ± 3.46 nM (n = 5); concentrations over 10 nM were observed at Stns. D2 and D3. The maximum [D-Mn] occurred in the surface water at all stations except for Stn. D1. The bottom depth was shallow (30 m) at Stn. D1; therefore, the decreasing trend of [D-Mn] with depth could not be observed. A maximum [D-Mn] at the surface is typical and well-recognized across the world ocean, including in the Arctic Ocean (Campbell and Yeats, 1982; Yeats, 1988; Middag *et al*., 2011). This trend can be attributed not only to riverine and atmospheric inputs, but also to photochemical reduction of Mn

oxides and light inhibition of microbial Mn oxidation (Sunda and Huntsman, 1988). Below the surface water, [D-Mn] tended to decrease with depth through the PSW. In the UHL, [D-Mn] began to increase with depth to a sharp peak in the UHL. The highest [D-Mn] (81.3 nM) was found in the near-bottom water at Stn. D2. A [D-Mn] over 57 nM was also found in the UHL at Stn. D3. The depths of [D-Mn] subsurface maxima generally correspond to the depths of [D-Fe] peaks in the UHL. As was noted for [D-Fe], the [D-Mn] in the UHL also gradually decreased with distance from the shelf break (Fig. 6, see section 4.3). In the AW, [D-Mn] began to decrease with depth with features of the scavenging-type distribution. The lowest value was observed in the deepest sample (500-m depth) in the AW at Stn. D5, which is consistent with expectations because it is the station farthest from the shelf break, and therefore farthest from the source of Mn in the study area.

The ranges of the [D-Ni], [D-Zn] and [D-Cd] were 2.66–9.28 nM, 0.58–6.04 nM and 0.11–0.99 nM, respectively (Figs. 5, 6 and Table 2); which also are values consistent with the previously reported values for this area (Cid *et al*., 2012). The relationships detected between salinity and [D-Ni], [D-Zn], [D-Cd] or [PO_4^{3-}] indicate that the maxima of [PO_4^{3-}] and the nutrient-type trace metals occurred in the UHL (Fig. 7). The ranges of [D-Ni], [D-Zn] and [D-Cd] within the UHL were similar between the Chukchi Shelf region and the Canada Basin, and correspond to the range of [PO_4^{3-}]. However, there were several disagreements with [PO_4^{3-}] distribution in the [D-Zn] and [D-Ni] data. In the PSW of the Canada Basin (Stn. 4), [D-Zn] and [D-Ni] had peaks near the surface (5-m depth), but this feature was not found in the [D-Cd] or [PO_4^{3-}]. In particular, [D-Ni] values in the PSW were generally high (6.37 ± 0.91 nM, n = 17) and similar to those in the UHL (7.46 ± 0.77 nM, n = 14). In the AW, [D-Ni], [D-Zn] and [D-Cd] were relatively uniform with depth, and there were no significant differences between sampling stations. Interestingly, [D-Ni] in the AW was considerably lower than in the other water masses, which was not the case for [D-Zn] and [D-Cd].

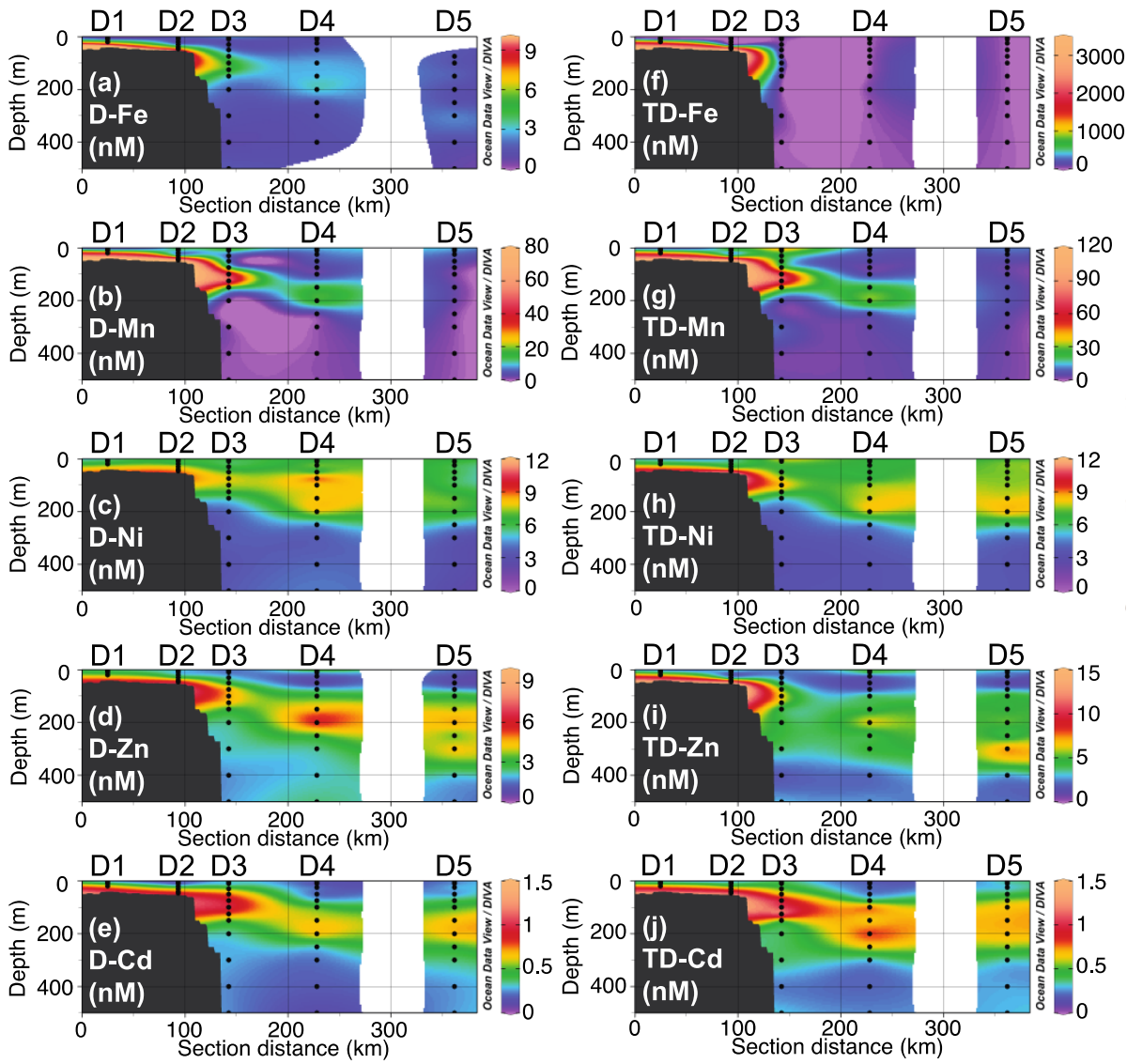

Fig. 5. Upper 500 m vertical sections of trace metal concentrations from Stns. D1 to D5; (a) D-Fe, (b) D-Mn, (c) D-Ni, (d) D-Zn, (e) D-Cd, (f) TD-Fe, (g) TD-Mn, (h) TD-Ni, (i) TD-Zn and (j) TD-Cd.

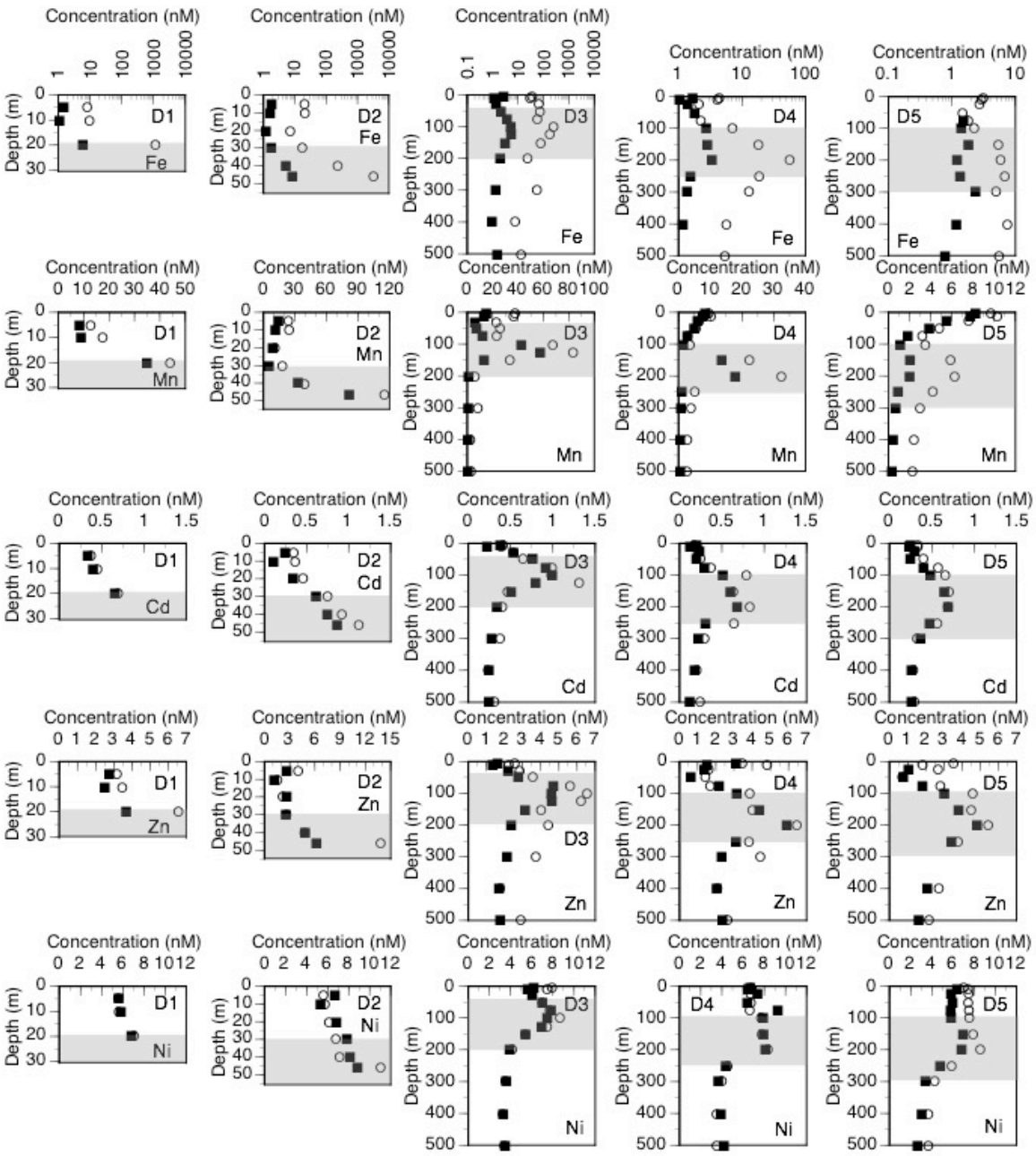

Fig. 6. Vertical distributions of trace metals for dissolved (filled square) and total dissolvable (open circle) fractions in each sampling station. Gray areas indicate the HL (combination of the UHL and LHL). Bottom depths at Stns. D1 and D2 are 30-m and 55-m, respectively.

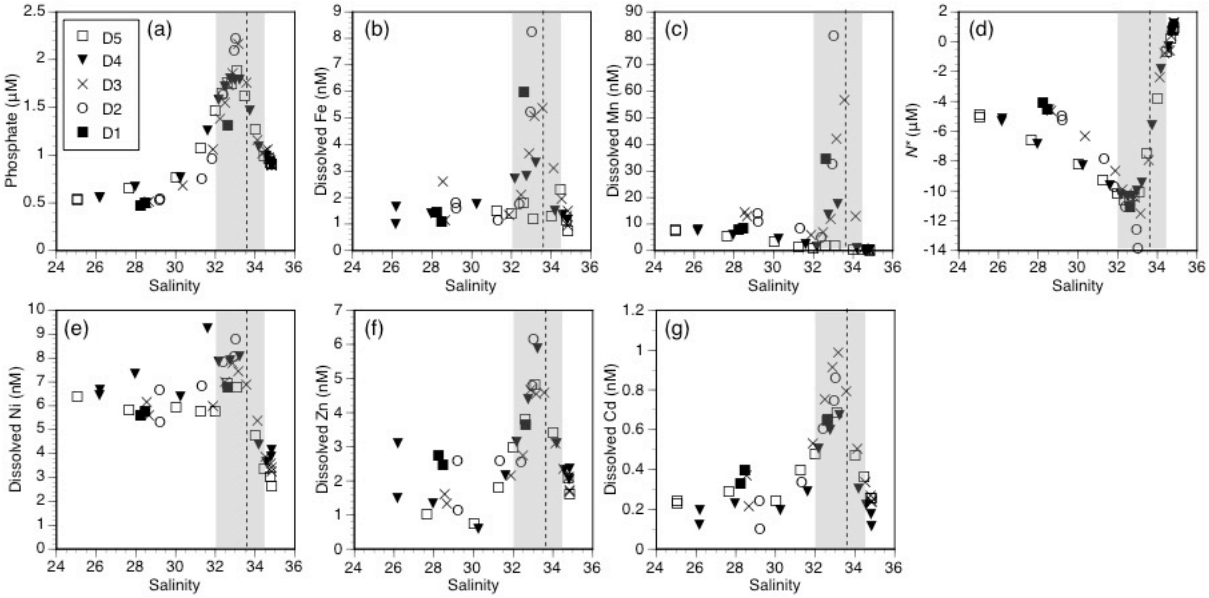

Fig. 7. Relationships between salinity and (a) [PO_4^{3-}], (b) [D-Fe], (c) [D-Mn], (d) *N**, (e) [D-Ni], (f) [D-Zn] or (g) [D-Cd]. The water masses were divided into 4 groups (PSW, UHL, LHL and AW) using salinity (see text). Gray areas indicate the HL (combination of the UHL and LHL). Broken lines indicate the boundary between the UHL and LHL.

3.3. Total dissolvable trace metals (TD-metals) in the Chukchi Sea and Canada Basin

The vertical distribution patterns were generally similar between D-metals and TD-metals, the maxima of which were also observed in the UHL (Figs. 5, 6, and Table 2). However, the behaviors of the dissolved and total dissolvable fractions were different between trace metals. In the case of Fe, the [TD-Fe] was much higher than [D-Fe] and varied substantially with depth (Fig. 6, Table 1); [TD-Fe] ranged from 1.47 to 3276 nM, and the ratio of dissolved to total dissolvable Fe fractions ([D-Fe]/[TD-Fe]) dramatically changed (0.003–0.841). Exceedingly high [TD-Fe] values were found from Stns. D1 and D2 (1173 and 3276 nM, respectively), and the [D-Fe]/[TD-Fe] ratios for these waters were low (0.003–0.005). In addition, [TD-Fe] as high as 253 nM was found in the UHL at Stn. D3 with low [D-Fe]/[TD-Fe] (0.02). In contrast, at Stn. D5, the maximum [TD-Fe] in the UHL decreased to 5.87 nM at 200-m depth, with a [D-Fe]/[TD-Fe] ratio for the sample increased to 0.21. These results suggest that Fe in the study area existed mainly in labile particulate form (LP-

Fe, [LP-Fe] = [TD-Fe] – [D-Fe]) in seawater with high Fe concentrations. [TD-Mn] ranged from 2.28 to 115 nM, and [D-Mn]/[TD-Mn] was also variable with depth at the same stations (0.082–0.99). The [TD-Mn] maxima were observed within the UHL at all stations except for Stn. D5, as was the case for [TD-Fe]. At Stn. D5, the highest [TD-Mn] was observed near the surface (5-m depth). The [TD-Mn] in the UHL decreased with distance from the shelf break from 115 nM (Stn. D2) to 6.26 nM (Stn. D5). Within ~ 270 km of the Chukchi Sea shelf break, both [TD-Fe] and [TD-Mn] in the UHL decreased dramatically by factors of ~ 480 and ~ 27, respectively. Near the bottom of the Chukchi Sea shelf break station (Stn. D2), where all of trace metals concentrations reached their maxima, the [D-metal]/[TD-metal] ratio of Mn (0.707) was much higher than that of Fe (0.003).

The maxima of [TD-Ni], [TD-Zn] and [TD-Cd] were also found in the UHL. Although the [D-metal]/[TD-metal] ratios ranged widely in this study (0.72–1.4 for Ni, 0.32–1.3 for Zn and 0.29–1.2 for Cd), the distribution pattern of [TD-Ni], [TD-Zn] and [TD-Cd] were similar to those of the respective dissolved fractions. These results indicate that at the time of the study, Ni, Zn and Cd mainly existed in dissolved forms in the western Arctic Ocean, which are consistent with the findings of Cid *et al*. (2012). Low [D-metal]/[TD-metal] ratios were observed near the bottom water and/or around subsurface chlorophyll maxima, which suggest that trace metal concentrations are affected by suspended sedimentary and/or biogenic particles. At some depths, [D-metal]/[TD-metal] ratios were higher than 1.0 (Table 1), which imply that recovery of these metals from unfiltered samples may not be sufficient.

4. Discussion

Our results show that both the dissolved and total dissolvable fractions of trace metals (Mn, Fe, Ni, Zn and Cd) had concentration maxima in the UHL in the western Arctic Ocean, and that especially high concentrations of Fe and Mn were observed in the Chukchi Sea continental shelf region (Figs. 5 and 6). These trends are generally consistent with the

findings of previous studies of this area (Nakayama *et al*., 2011; Nishimura *et al*., 2012; Cid *et al*., 2012; Aguilar-Islas *et al*., 2013; Hioki *et al*., 2014). However, we found that the concentrations of [D-Fe] from our samples were higher than those of Hioki *et al*. (2014), whose seawater samples were collected on the same cruise (section 4.1). In the following sections, we discuss the sources of trace metals (section 4.2), offshore transportation (section 4.3) and the implications of these trends in the Chukchi Sea and Canada Basin (section 4.4).

4.1. Comparison of Fe concentration results with previous study results

Reported [D-Fe] and [TD-Fe] values from previous studies of the western Arctic Ocean have varied widely: 0.36–33.1 nM and 0.8–89000 nM, respectively (Nakayama *et al*., 2011; Nishimura *et al*., 2012; Cid *et al*., 2012; Aguilar-Islas *et al*., 2013; Hioki *et al*., 2014). Our dataset for both [D-Fe] and [TD-Fe] fall within these ranges, although the concentration we report are higher than those of Hioki *et al*. (2014) (Fig. 8). As mentioned in the method section, the seawater samples analyzed for this study and those analyzed by Hioki *et al*. (2014) were obtained from the same sampling bottles simultaneously. However, values of [D-Fe] in this study are 1.6 ± 0.5 (n = 37) times higher than those of Hioki *et al*. (2014) (Fig. 8). The chelating resin preconcentration and ICP-MS method (adapted from Sohrin *et al*., 2008) was used to measure trace metals simultaneously in this study, whereas Hioki *et al*. (2014) used an automated Fe analyzer with a combination of chelating resin preconcentration and a luminol–hydrogen peroxide chemiluminescence detection method (Obata *et al.*, 1997). Nonetheless, the Fe detection methods of both studies were applied successfully with reference seawaters, such as the SAFe and GEOTRACES standard waters. The profiles produced by both studies are not erratic but oceanographically consistent. We believe that both datasets represent the chemically-labile dissolved fractions of Fe in seawater. However, the sample preservation periods and degree of acidification were significantly different between these two studies; the seawater samples used in this study were stored for over two

years at pH 1.5–1.6, whereas the samples used by Hioki *et al*. (2014) were stored at pH 1.7–1.8 for three months prior to analyses. Based on the low [D-Fe]/[TD-Fe] ratios determined in this study, there may be abundant colloidal particles in the western Arctic Ocean, especially in the Chukchi Sea continental shelf/slope region. Previous studies also observed higher concentrations of TD-Fe compared to D-Fe (Nakayama *et al*., 2012; Cid *et al*., 2012; Aguilar-Islas *et al*., 2013; Hioki *et al*., 2014). Because the preservation period for seawater samples was much longer for this study, some chemically labile components were released from colloidal particles in the filtered seawater samples over that two-year period. Further research is required to evaluate the impact of sample preservation periods on trace metal concentrations, especially for samples from coastal shelf regions such as the Chukchi Sea.

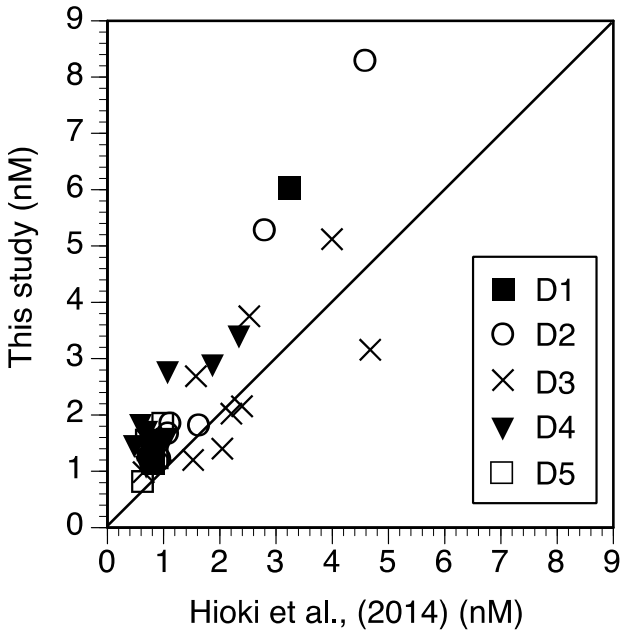

Fig. 8. Comparison of [D-Fe] in the western Arctic Ocean between Hioki *et al.* (2014) and this study. A solid line indicates 1:1 ratio.

4.2. Sources of trace metals in the western Arctic Ocean

Our results show that all of the analyzed trace metals (Fe, Mn, Ni, Zn and Cd) had characteristic distributions in the western Arctic Ocean in the late summer of 2012, and generally these trace metals were present at high concentrations; halocline water was the

most enriched in Mn, Ni, Zn, Cd, Fe and nutrients. The trends in the relationships between D-metals and PO_4^{3-} concentrations reflect the distinct properties of each trace metal in the ocean interior (Fig. 9). [D-Ni], [D-Zn] and [D-Cd] were more strongly correlated with [PO_4^{3-}] than were [D-Fe] or [D-Mn], which suggest that the distributions of D-Ni, D-Zn and D-Cd were generally controlled by the internal biogeochemical cycles of the ocean interior that also affect PO_4^{3-}, whereas the distributions of D-Fe and D-Mn were more strongly influenced by external sources and/or removal of trace metals from the water column. Similar properties were also suggested based on studies of other continental shelf regions such as the central California Current System (Biller and Bruland, 2013).

Iron is well-known as a controlling factor of phytoplankton stocks in a wide range of oceanic environments (e.g., Moore *et al.*, 2013). However, the growth of phytoplankton in this study area is generally recognized as limited by nitrogen during the summer, as discussed above. Our results suggest that [D-Fe] in the PSW in the western Arctic Ocean was generally higher than those in other Arctic basins, such as the Nansen Basin and the Amundsen Basin (Klunder *et al.*, 2012a), but similar to those of adjacent areas such as the northern Bering Sea shelf (Nishimura *et al.*, 2012). In the central Arctic Ocean, Klunder *et al*. (2012b) found minima of [D-Fe] near the surface, which suggest depletion of D-Fe by phytoplankton growth. For this study, we calculate an index *Fe** (*Fe** = [D-Fe] – 0.47 [PO_4^{3-}]) to quantify the degree of Fe limitation on phytoplankton growth relative to [PO_4^{3-}] (Parekh *et al.*, 2005). Positive *Fe** generally implies adequate [D-Fe] to support the complete biological utilization of PO_4^{3-}, while negative *Fe** indicates a Fe deficit relative to PO_4^{3-} (Parekh *et al.*, 2005). In this study, *Fe** in all samples had positive values (0.32–7.21, n = 39), which suggest that Fe was replete for phytoplankton growth even relative to PO_4^{3-} in the western Arctic Ocean during late summer 2012. Furthermore, among the water masses considered in this study, *Fe** was lowest in the AW, which emphasizes the importance of the Pacific-origin waters that pass over the continental shelf as a major source of Fe in the western Arctic Ocean.

Previous studies of this region have suggested several potential external sources of trace metals: re-suspension of sediment particles from the shelf, sea-ice melting, river discharge and water inflow from the Bering Strait (Nishimura *et al*., 2012; Cid *et al*., 2012; Aguilar-Islas *et al*., 2013; Hioki *et al*., 2014). As discussed above, Hioki *et al*. (2014) have demonstrated a scheme of the sources and processes responsible for lateral transport of Fe in the western Arctic; the cold and dense waters that characterize the UHL have high levels of Fe, nutrients and dissolved organic matter from interaction with shelf sediment and from brine production by the formation of sea ice in the fall and winter. Because there is a positive correlation between [D-Fe] and [D-Mn] in the UHL (Fig. 10), similar processes may also operate in D-Mn distribution, especially in the UHL. Among the potential external sources mentioned above, sedimentary input was the most important source of all trace metals, especially Fe and Mn. In the bottom layer over the sea floor, D-Fe and D-Mn are expected to be supplied in their reduced forms, Fe(II) and Mn(II), from the suboxic and/or anoxic sediments. Reduced Fe(II) is then oxidized to the less soluble Fe(III) in the oxic water column, and some are complexed with the natural organic ligands such as humic substances (Lohan and Bruland, 2008). Recently, many studies have further indicated that the release of Fe(II) from reducing continental shelf sediments may be an important source of Fe in coastal waters (Pakhomova *et al*., 2007; Noffke *et al*., 2012; Chever *et al*., 2015). However compared to Fe(II), reduced Mn(II), is more slowly oxidized to insoluble Mn(III) and Mn(IV) oxides in oxic seawater (Millero *et al*., 1987; Sunda and Huntsman, 1987, 1990; von Langen *et al*., 1997; Santana-Casiano *et al*., 2005; Morgan, 2005). The positive correlation between [D-Fe] and [D-Mn] in the UHL suggests that the binding of Fe with organic ligands and the removal of remaining Mn occur at similar time scales in the UHL. The removal and transportation processes will be discussed in section 4.3.

In the PSW, the inflow of low-salinity Pacific-origin water from the Bering Strait and local fresh water inputs such as sea-ice meltwater and river water may be important sources

of trace metals in the study area in addition to the upward inputs from sediment. For Fe, although [D-Fe] and [TD-Fe] in the Canada Basin PSW were lower than those in the Chukchi Sea shelf and slope regions, they were still higher than those of other typical oceanic regions, such as subarctic North Pacific (e.g., Kondo *et al*., 2012) and the central Arctic basins (e.g., Klunder *et al*., 2012a). Over the last 20 years, the freshwater discharge from major Arctic rivers has increased (Doxaran et al., 2015 and references therein), the accumulation of significant amount of freshwater has been observed in the Beaufort Gyre of the Canada Basin (e.g., Morrison et al., 2012). According to the calculated fractions of meteoric water and sea-ice meltwater in the surface water, the fraction for meteoric water was higher (6-18%) than that for sea-ice meltwater (2-8%). It suggests that the meteoric water was the major source of freshwater in this study area. In this region, there are several large rivers that can affect the properties of water in the Chukchi Sea region, including the Mackenzie River and the Yukon River. The Mackenzie River, which is the largest and longest river that flows into the Beaufort Sea, has a water discharge of 249–333 km^3/year; its river water is rich in suspended material (Dittmar and Kattner, 2003). Cid *et al*. (2012) reported that the concentrations of all trace metals in the Mackenzie Trough in 2002 were higher than those in the Canada Basin for both the dissolved and total dissolvable fractions. The Yukon River flows from British Columbia through Alaska and into the northeastern Bering Sea shelf with an average water discharge of ~ 198 km^3/year that varies seasonally (Wickland *et al.*, 2012), which could account for ~ 8% of the freshwater input into the Arctic Ocean (Aagaard and Carmack, 1989). Nishimura *et al*. (2012) observed high [D-Fe] in low-salinity surface water in the Yukon River estuarine region (> 10 nM) and the Bering Strait (~ 5–10 nM). Moreover, there are several large rivers in the Siberian shelves of the Arctic Ocean, such as the Lena River and Kolyma River. The input of fresh water from the Lena River could strongly impact Mn input in the Laptev Sea estuary (Middag *et al*., 2011). The Kolyma River is located in northern Siberia with a mean water discharge of 122 km^3/year (Rachold et al., 2004). Although the

concentrations of trace metals are unknown, it has been reported that this river contains vast reserves of carbon in Pleistocene-aged permafrost soils (Griffin et al., 2011). Not only the meteoric water, but also sea-ice melting also strongly influences trace metal distributions in the western Arctic. In late summer 2012, the surface area of ice covering in the Arctic Ocean reached its lowest extent in recorded history (Wood *et al*., 2015), resulting that significant portion of sea-ice meltwater was found in the PSW in this study area. Previous studies have suggested that melting sea ice is a plausible source of Fe in the Arctic (Measures, 1999; Tovar-Sánchez *et al.*, 2010), as well as in the Sea of Okhotsk (Kanna *et al.*, 2014), the Bering Sea (Aguilar-Islas *et al.*, 2008) and the Antarctic (e.g., Noble *et al.*, 2013). Measures (1999) reported that the concentrations of Fe and Al in surface seawater in the Arctic Ocean were elevated near large masses of sea ice that contained entrained sediments. Tovar-Sánchez *et al*. (2010) determined the concentrations of trace metals (Fe, Mo, Ni, Zn, V, Cu and Co) and nutrients in seawater and multilayered ice along the Greenland current and the Fram Strait and showed that the sea ice was more enriched in these trace metals relative to the surface waters. Noble *et al*. (2013) investigated the distribution of trace metals (Mn, Fe, Al, Co, Cu and Cd) under the McMurdo Sound seasonal ice beneath in the Ross Sea and found that the all metals except for Cd had extremely high concentrations in the shallowest samples. In the present study, we also observed increases in both [D-metals] and [TD-metals] in the surface water at the northernmost station (Stn. D5), with the exception of Cd. These findings suggest that sea ice near the continental margins in particular could supply these trace metals to the water column via melting. Because our study area covers a shelf region, and because the PSW was most likely strongly influenced by meteoric water and inflow from the Bering Strait and the Chukchi Sea continental shelf, sea ice in this area presumably contained terrestrial materials. Indeed, the [D-Fe]/[TD-Fe] ratio in the surface water (5-m depth) was low (0.07–0.38), which suggests that the particulate form was the dominant fraction of Fe in the surface water. Therefore, these sources of freshwater input from rivers and Pacific inflow

are inferred to have significant influence on trace metal distributions in the western Arctic via the Beaufort Gyre and/or the formation of sea-ice in the fall and winter. Altogether, the existence of various sediment-rich input sources likely sustained the high surface concentrations of trace metals observed in the western Arctic Ocean.

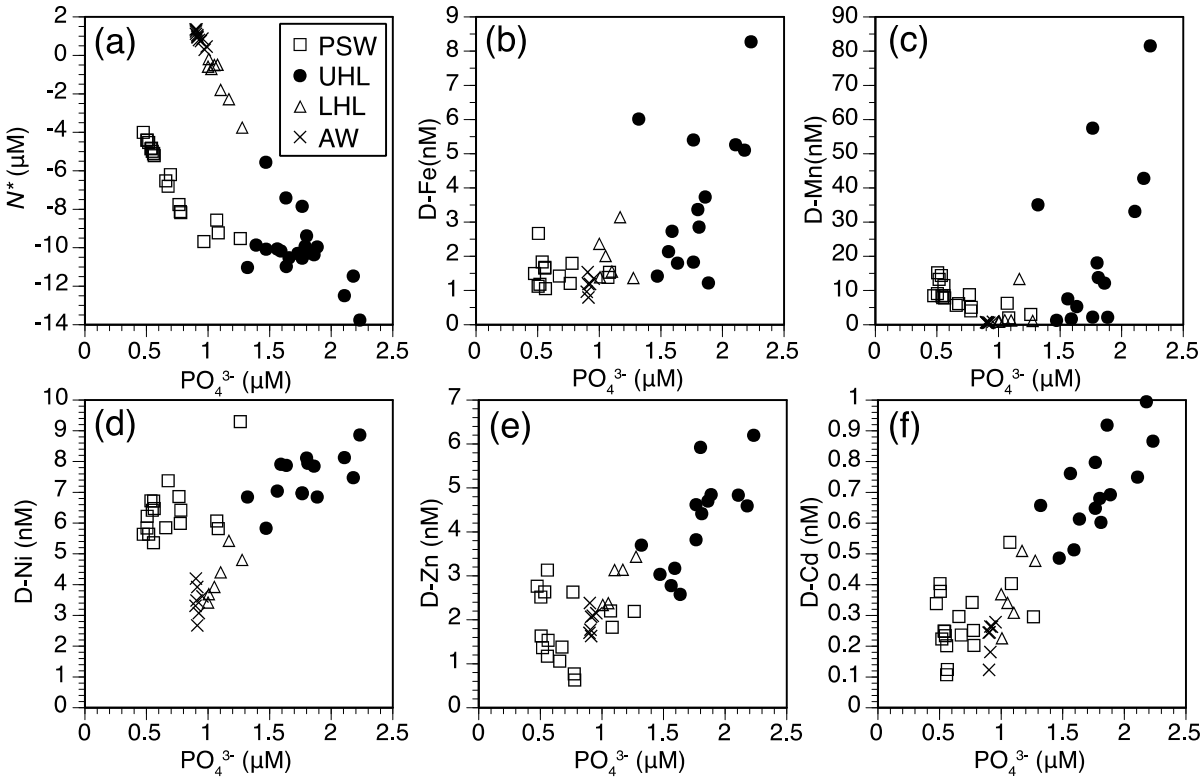

Fig. 9. Relationships between [PO_4^{3-}] and (a) *N**, (b) [D-Fe], (c) [D-Mn], (d) [D-Ni], (e) [D-Zn] or (f) [D-Cd].

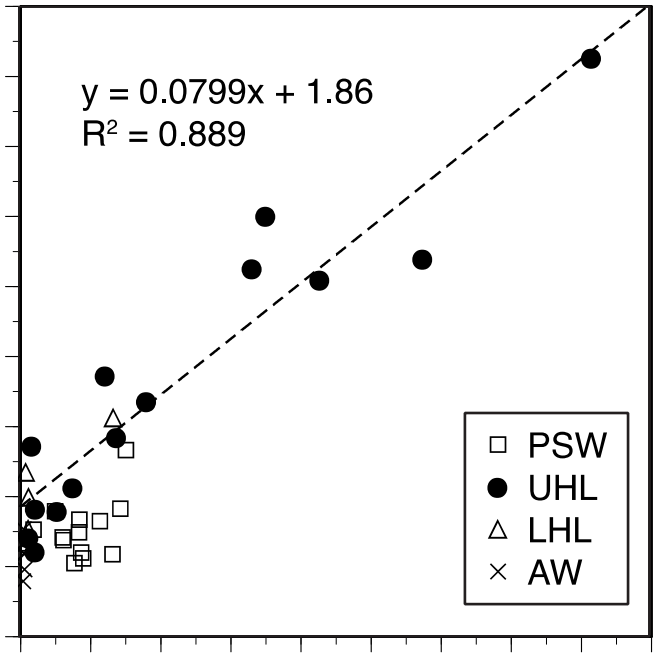

Fig. 10. Relationships between [D-Fe] and [D-Mn]. A broken line indicates the regression line in the UHL.

4.3. Transport of Fe and Mn within the HL in the western Arctic Ocean

Within the HL, concentration maxima were identified for both D-metals and TD-metals of all five trace metals included in this study. For Fe and Mn, their subsurface maxima in the UHL were distinct from those in other Arctic basins (i.e., the Nansen, Amundsen and Makarov Basins) and shelf regions (the Barents, Kara and Laptev Seas) (Middag *et al*., 2011; Thuróczy *et al.*, 2011). The relationships between the distance from the shelf break (Stn. D2) and the natural logarithm of [D-metals] or [TD-metals] in the HL reflect the characteristics of transport of each trace metal (Fig. 11). In this study, the concentrations of Fe and Mn (for both the dissolved and total dissolvable fractions) decreased logarithmically with increasing distance from the shelf break in both the UHL and LHL, whereas the change in [PO_4^{3-}] was small. This relationship suggests that scavenging processes within the UHL controlled the transports of Fe and Mn. The [TD-Fe] decreased dramatically with distance compared to [D-Fe] in this layer, which indicates that labile particulate Fe was preferentially removed from

the water column. In contrast, [TD-Mn] decreased more slowly than [TD-Fe], but [D-Mn] decreased faster than [D-Fe] (Fig. 11). To evaluate the phase distributions of Fe and Mn during lateral transportation, we calculated [LP-Fe]/[D-Fe] and [LP-Mn]/[D-Mn] ratios in seawater, where [LP-Mn] = [TD-Mn] – [D-Mn] (Fig. 12). The [LP-Fe]/[D-Fe] ratio in the UHL decreased logarithmically against distance from the shelf break, whereas the [LP-Mn]/[D-Mn] ratio gradually increased with distance. These results reflect the differing behavior of Fe and Mn in the transport processes of this region. For Fe, the [TD-Fe] decreased quickly via removal of LP-Fe from the water column, whereas the [TD-Mn] decreased more slowly through the transformation of D-Mn to LP-Mn. Fig. 11 also shows that [D-Fe] and [D-Mn] in the UHL would decrease to the levels observed in the AW within ~ 350 km and ~ 390 km north of Stn. D2, respectively. The accumulation of [NH_4^+] in the UHL was also observed, and there were positive correlations between [NH_4^+] and [D-Fe]/[D-Mn] (data not shown). Brown *et al*. (2015) investigated the stable isotopes of oxygen (^{16}O and ^{18}O) and nitrogen (^{14}N and ^{15}N) of NO_3^- in the Chukchi Sea shelf region, and the results suggested that the main source of the NH_4^+ accumulated in the near-bottom water was sedimentary input, not degradation of organic matter in the water column. Therefore, the observed increases in [NH_4^+] in the near-bottom water were most likely derived from the sediments of the Chukchi Sea continental shelf; the time scale for its removal from the water column was similar to those for D-Fe and D-Mn during our observational period. Considering the dispersion of the slopes for D-Mn and D-Fe (Fig. 11), there were no significant differences between D-Mn and D-Fe. A similar result was also calculated for D-Fe from the dataset of Hioki *et al*. (2014). These results further suggest that the elevated D-Fe and D-Mn levels were removed within the similar scales of time. It has been suggested that Fe(II) is oxidized rapidly within minutes to hours in oxygenated water (Santana-Casiano *et al.*, 2005), whereas the oxidation of soluble Mn(II) by Mn-oxidizing bacteria proceeds at was much slower rate on a scale from hours to days (Sunda and Huntsman, 1988). Our results do

not follow the general chemical properties of Fe and Mn with respect to the oxidation kinetics described above, which suggest the existence of moderate scavenging mechanisms for Fe(III) in the study area. In this case, we can propose that a high [D-Fe] was sustained in the HL because of the presence of organic ligands such as humic substances. It has been demonstrated that humic substances are important sources of organic ligands in coastal areas (e.g., Laglera *et al*., 2011). Hioki *et al*. (2014) investigated the distribution of humic-like fluorescent dissolved organic matter (humic-FDOM) as an index for humic substances, and found that the maxima of humic-FDOM occurred in the HL in the western Arctic Ocean. Furthermore, Yamada *et al.* (2015) investigated the distribution of transparent exopolymer particles (TEP) using a 0.4-μm pore-size polycarbonate filter with samples collected during the same cruise as the samples in the present study and observed that the ratios of TEP carbon to total particulate organic carbon (POC) were generally high in the shelf and slope regions in the study area. This finding suggested that particles containing large amounts of TEP were produced in the shelf region and transported offshore. Furthermore, because TEP is produced through flocculation of marine biogenic polysaccharides, which are also recognized as organic ligands for Fe (Stolpe and Hassellöv, 2010), this finding indicates that the organic ligands for Fe may also be supplied from the sediment and biological production on the Chukchi Shelf and transported offshore. In the western Arctic Ocean, Aguilar-Islas *et al.* (2013) also demonstrated the relationship between the natural logarithm of Fe concentration and the distance from the shelf in halocline waters based on observations made in the summer of 2010, and reported the resulting equation: Ln[D-Fe] = -0.0026 × [distance from 100-m isobaths (km)] + 0.9836. Although the averaged absolute value of the slope from this study was slightly higher than that reported by Aguilar-Islas *et al*. (2013), there was no significant difference when the unevenness of [D-Fe] in the UHL in our study was considered (Fig. 11). In late summer 2012, it was reported that northwesterly winds flowing in the northern part of an extended Siberian High transported oligotrophic water into the Beaufort Gyre, which

circulated it toward our study area (Watanabe *et al.*, 2015). An unusually large warm-core eddy (~ 100 km in diameter) had been observed in the Canada Basin in late summer 2010 (Nishino *et al.*, 2011), which suggested that the offshore transports of nutrients and Fe could have been enhanced by the eddy (Nishino *et al.*, 2011; Aguilar-Islas *et al.*, 2013). However, because our sampling sites were located too far to the east of the study area of Aguilar-Islas *et al.* (2013) to investigate the effects of this eddy, further research is still required to evaluate the impacts of hydrographic and meteorological changes to the transport of Fe in the western Arctic Ocean.

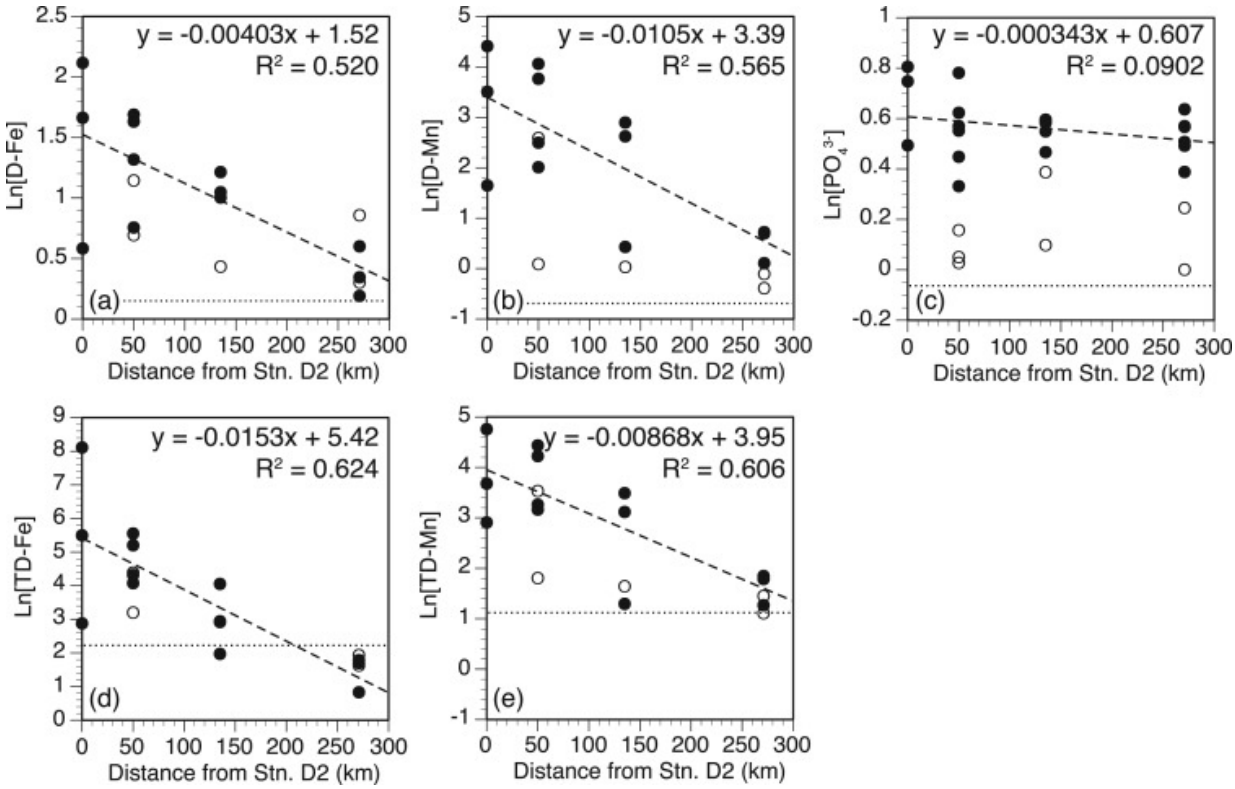

Fig. 11. Logarithmic changes in concentrations of (a) D-Fe, (b) D-Mn, (c) PO_4^{3-}, (d) TD-Fe and (e) TD-Mn in the UHL (closed circles) and LHL (open circles) against the distance from Stn. D2. Each broken line indicates the regression line in the UHL. The dotted line indicates the average concentration of each trace metal in the AW.

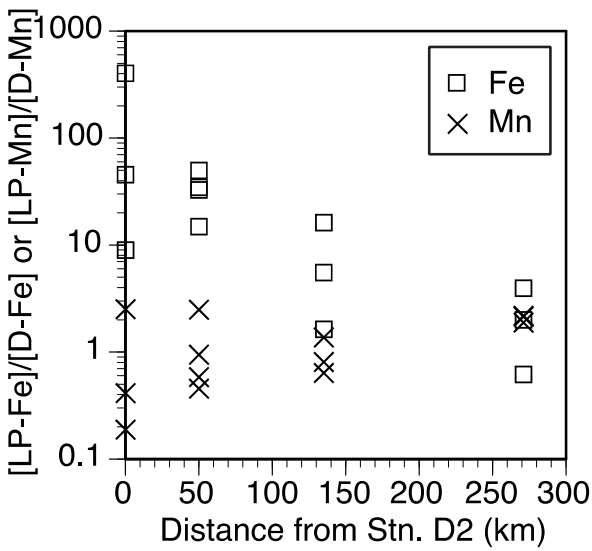

Fig. 12. Changes in the ratio between labile particulate and dissolved concentrations for Fe ([LP-Fe]/[D-Fe]) or Mn ([LP-Mn]/[D-Mn]) in the UHL against the distance from Stn. D2.

4.4. Implications of nutrient-type trace metal behaviors in the western Arctic Ocean

Our results suggest that the elevated Ni, Zn and Cd concentrations in the HL may extend across the Canada Basin from the Chukchi Sea shelf break area. The relationships between salinity and D-metals/PO_4^{3-} indicate that the maximum concentrations of both PO_4^{3-} and D-metals were observed in the UHL ($\sigma_\theta \approx 26.5$) (Fig. 7). The trends in the relationships between concentrations of D-metals and PO_4^{3-} reflect the distinct properties of each trace metal in the ocean interior (Fig. 9). As discussed in section 4.3, the variation in [PO_4^{3-}] within the UHL was small over the study area (Fig. 11). Similarly small variations were also observed in [D-Zn], [D-Ni] and [D-Cd] (data not shown). It has been suggested that most of the regeneration of organic matters occurs over the Chukchi Sea shelf and slope regions and in the shelf sediments, whereas abyssal regeneration in the Canada Basin was minor (Codispoti *et al*., 2005). This trend would imply that Ni, Zn and Cd accumulated on the Chukchi Sea shelf in the UHL with nutrients and could be transported northward offshore via

the UHL at least as far as ~270 km north of the shelf break while maintaining high concentrations. Indeed, previous studies have found that the concentration maxima of Ni, Zn, and Cd occurred in the HL of the Canada Basin near the Canadian Arctic Archipelago (Yeats, 1988; Yeats and Westerlund, 1991), which support the interpretation that the elevated Ni, Zn and Cd concentrations in the HL extend across the Canada Basin from the Chukchi Sea shelf break area. [D-Ni], [D-Zn] and [D-Cd] correlate more strongly with [PO_4^{3-}] than [D-Fe] or [D-Mn], which suggest that, like PO_4^{3-}, the distributions of D-Ni, D-Zn and D-Cd were generally controlled by internal biogeochemical cycles of the ocean interior. This behavior has also been proposed for other continental shelf regions such as the central California Current System (Biller and Bruland, 2013). However, there were differences in the strengths of the correlations between [PO_4^{3-}] and [D-Ni], [D-Zn] and [D-Cd]. [D-Cd] showed the strongest correlation with [PO_4^{3-}], and [D-Ni] the weakest correlation, with [D-Zn] in the middle.

The high [D-Cd]/[TD-Cd] ratio and positive correlation between [D-Cd] and [PO_4^{3-}] suggest that the distribution of Cd was most likely to be controlled by internal biogeochemical cycles in the study area, which is consistent with the findings of Cid *et al.* (2012). The strong positive correlation between [D-Cd] and [PO_4^{3-}] was also reported by Yeats and Westerlund (1991), who investigated trace metal (Cd, Zn, Cu and Ni) distributions near the Canadian Arctic Archipelago in the Canada Basin. Cd can act either as a nutrient or as a toxin; therefore it influences phytoplankton growth. Especially in the coastal areas in industrialized regions, rivers are thought to be the most important source of Cd after atmospheric input (Lambelet *et al*., 2013 and references therein). Our results indicate the [D-Cd] in the PSW ranged from 0.11 to 0.47 nM, which are similar level to those in the coastal seas of the Siberian Shelf (0.02–0.46 nM) (Lambelet *et al*., 2013). Off the coast of central California, similar [D-Cd] has been reported (0.05–0.87 nM) (Biller and Bruland, 2013). Overall, the [D-Cd] in the surface water of the western Arctic Ocean was high relative to

those in the oligotrophic open oceans such as the North Pacific (~0.002 nM) (e.g., Bruland, 1980), but it is similar to [D-Cd] in coastal areas. Cullen (2006) suggested that preferential uptake of Cd in surface seawater under Fe limitation could cause a 'kink' in the relationship between [D-Cd] and [PO_4^{3-}] that results in a lower [D-Cd]/[PO_4^{3-}] ratio (e.g., < 0.21 × 10^{-3}). In the present study there was no kink in this relationship, which is consistent with our discussion of *Fe** in section 4.3 where it was explained that [D-Fe] was replete in the surface water in this area. The [D-Cd]/[PO_4^{3-}] ratios were higher than 0.34 × 10^{-3} at all stations (the minimum coefficient of determination was 0.93), which are similar to the values for that ratio in the eastern North Pacific (Bruland, 1980).

The ranges of both [D-Zn] and [TD-Zn] in this study were similar to those in the earlier study in the western Arctic Ocean (Cid *et al*., 2012). It has previously been reported that the [D-Zn] correlates more strongly with [$Si(OH)_4$] (i.e., correlation coefficient = 0.996) than with [PO_4^{3-}] or [NO_3^-] in the ocean (e.g., Bruland, 1980). In the western Arctic Ocean, [D-Zn] and [$Si(OH)_4$] were generally correlated, but the correlation coefficient was relatively poor: [D-Zn] (nM) = 0.10 [$Si(OH)_4$] (μM) + 1.19 (R^2 = 0.801) (Fig. 13). The slope value (Zn/Si, 0.10) was higher than those reported from the North Atlantic (0.058) (Roshan and Wu, 2015), North Pacific (0.054–0.067) (Kim *et al.*, 2015 and references therein) and Bering Sea (0.078) (Fujishima *et al.*, 2001). The Zn/Si ratio of the Bering Sea was slightly higher than those of the North Pacific. Based on the influence of the Pacific-origin water entering through the Bering Strait into the western Arctic Ocean, the Zn/Si slope was likely modified during the process of transport from the Bering Sea to the Chukchi Sea shelf region. We found that both [D-Zn] and [TD-Zn] were elevated in near-bottom water at Stns. D1 and D2, where Fe and Mn also reached their maxima. In these samples, the [TD-Zn] values were especially high; the concentrations of labile particulate Zn (LP-Zn, [LP-Zn] = [TD-Zn] − [D-Zn]) near the bottom at Stns. D1 and D2 were 2.88 nM and 7.64 nM, respectively. As a result, the [D-Zn]/[TD-Zn] ratios for these samples were as low as 0.45–0.56. Although the [D-metal]/[TD-

metal] ratios for Zn were generally higher than those of Fe and Mn, they tended to be lower than those of Ni and Cd in the study area. Trefly *et al*. (2014) reported the concentrations of trace metals (including Fe, Mn, Ni, Zn and Cd) in surface sediments in the northeastern Chukchi Sea; the Zn/Fe and Zn/Mn ratios in these surface sediments were calculated to be approximately 0.0021 and 0.17, respectively. These values were similar to the [LP-Zn]/[LP-Fe] ratios (0.0023–0.0024) and [LP-Zn]/[LP-Mn] ratios (0.23–0.31) of the near-bottom waters at Stns D1 and D2. These results indicate that not only Fe and Mn, but also Zn were supplied to near-bottom water from continental shelf sediment in the Chukchi Sea. The [LP-Zn]/[LP-Fe] and [LP-Zn]/[LP-Mn] ratios in the UHL increase with distance from the shelf break (Stn. D2), which suggest faster removal of LP-Fe and LP-Mn from the water mass compared to LP-Zn. In addition to sedimentary input, the influences of fresh water inputs such as melting sea-ice and river waters may also be a reason for the weak correlation between [D-Zn] and [$Si(OH)_4$], as well as the high slope value. Both [D-Zn] and [TD-Zn] had peaks near the surface in the Canada Basin (Stns. D4 and D5). Because sea ice is not the source of the $Si(OH)_4$ in seawater in the Arctic Ocean (Tovar-Sánchez *et al*., 2010), the increase in Zn concentration in the PSW was likely derived from the sea-ice melting over the summer.

Ni is classified as a nutrient-type trace metal and has high [D-Ni]/[TD-Ni] ratios in our dataset. However, the relationship between [D-Ni] and [PO_4^{3-}] showed more scattering compared to those between [D-Cd] or [D-Zn] and [PO_4^{3-}] (Fig. 9), which suggests that phytoplankton uptake and remineralization of settling particles have only minor effects on the distribution of D-Ni in the study area. It is likely that the high [D-Ni] in the PSW (6.19 ± 0.56 nM, n = 13) relative to other areas, such as the North Pacific (Bruland, 1980; Fujishima *et al*., 2001) and the central California Current system (Biller and Bruland, 2013), caused the scattering in the relationship between [D-Ni] and [PO_4^{3-}]. The concentration of Ni in the sea ice has been reported to be higher than that of the surrounded seawater, as have the

concentrations of other trace metals such as Fe, Mn, Co, Cu and Zn (Tovar-Sánchez *et al*., 2010; Noble *et al*., 2013). Therefore, the [D-Ni] has remained high in the PSW of the Canada Basin. Furthermore, similar [D-Ni] values were observed in the Bering Sea and its shelf area, including in the Bering Strait (Fujishima *et al.*, 2001; Cid *et al.*, 2011, 2012). Therefore, high [D-Ni] in the Chukchi Sea PSW may be derived from the supply of the Pacific-origin water that passes through the Bering Strait. Interestingly, we found that the [D-Ni] was inversely proportional to N^* (Fig. 14); the coefficient of determination for this relationship (R^2 = 0.812) was higher than those for relationships between N^* and the macro-nutrients PO_4^{3-}, NO_3^- and $Si(OH)_4$, whereas no linear relationships were observed between N^* and the other trace metals in the study. Accumulations of D-Ni and NH_4^+ were observed in negative N^* waters where the influence of sedimentary denitrification and/or anammox was strong. These observations were consistent with those of previous studies that reported elevated [NH_4^+] in near-bottom water in the Chukchi Sea shelf and slope regions (Codispoti *et al*., 2005; Connelly *et al*., 2014). Because water column denitrification only occurs when dissolved oxygen concentration is below 2–4 μM (e.g., Devol, 1978), the negative N^* values in this study likely indicate the influence of sedimentary denitrification and/or anammox or the preferential release of PO_4^{3-} from the sediment. These findings imply that D-Ni in near-bottom water was supplied during early diagenesis of the surface sediment and transported offshore within the HL. In biological metabolism, Ni is associated primarily with Ni-SOD and urease (Dupont *et al*., 2008a, b). Urease is an amidohydrolase with Ni in the active site that catalyzes the dissociation of urea into NH_4^+ and carbon dioxide, which provides a source of nitrogen for the organism. Most phytoplankton, including cyanobacteria, coccolithophores, dinoflagellates, cryptophytes and prasinophytes, use urease (Dupont *et al.*, 2010). Furthermore, metagenomic analysis has revealed that Arctic archaea and small prokaryotes possess the urease gene in high abundance, which suggests that their nitrification and autotrophic growth may be fueled by urea in the Arctic Ocean (Alonso-Saez *et al.*, 2012).

Connelly *et al*. (2014) reported that major microbial incorporation of nitrogen shifted from NH_4^+ in the summer to urea in the winter during sea-ice formation. Although the reason why the [D-Ni] and *N** show a strong linear relationship remains unclear, the presence of high [D-Ni] can sustain the organisms' use of urea in this study area. Further study is required to elucidate the role of Ni in the nitrogen cycle in the western Arctic Ocean.

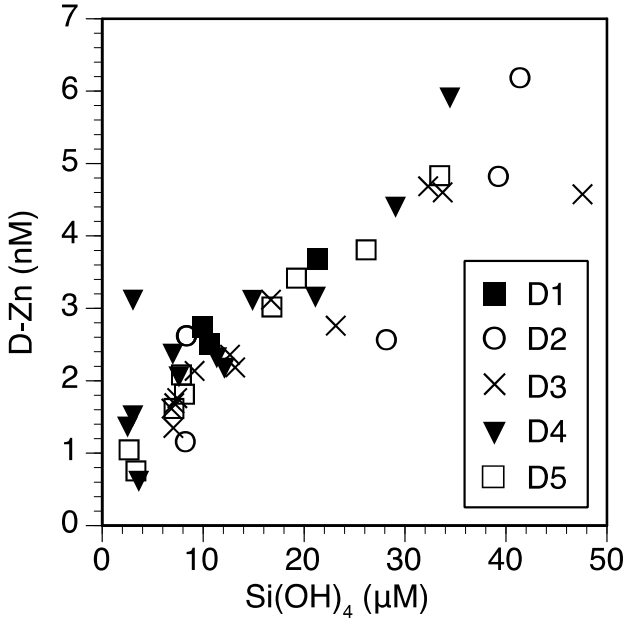

Fig. 13. Relationship between [$Si(OH)_4$] and [D-Zn].

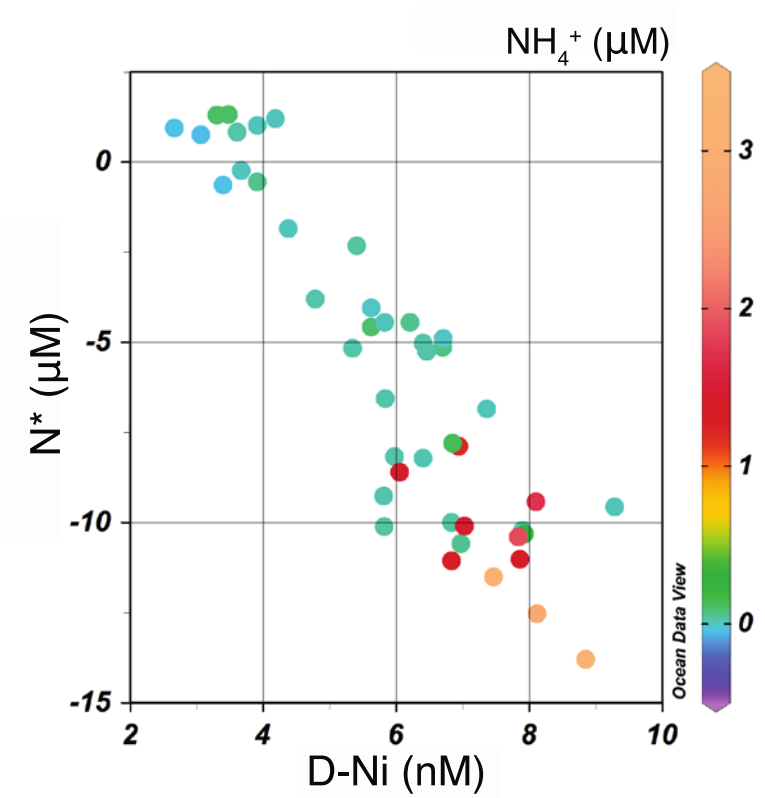

Fig. 14. Relationship between [D-Ni] and *N**. The color of each point indicates [NH_4^+]. The [NH_4^+] accumulation was only found in high [D-Ni] and low *N**.

5. Conclusions

Our results indicate that the concentrations of trace metals (Mn, Fe, Ni, Zn and Cd) were generally high in the Chukchi Sea continental shelf and slope regions, particularly within the UHL. The HL contributes to the unique distribution patterns of trace metals in the western Arctic Ocean. In this region, not only does the Pacific-origin inflow water from the Bering Strait contain high concentrations of trace metals, but there are also various additional sources of trace metals that may contribute to this enrichment, such as continental shelf sediments, river water discharge, melting sea ice and remineralization of organic matter. It is likely that the trace metals-rich halocline water is transported offshore and mixed with ambient water masses. Nonetheless, it is important to identify and evaluate the differences in each vertical profile for different trace metals. For Fe and Mn, the balance between major

benthic input and rapid removal by scavenging must be considered to understand their patterns of distribution. In contrast, the elevated Ni, Zn and Cd, which existed as mainly dissolved forms, were transported further offshore from the Chukchi Sea shelf break to Canada Basin within the UHL. In this study, we also explored the possibility of dissociation of refractory colloidal Fe during the long-term preservation of our samples; this issue is important for estimation of the Fe budget in the Arctic Ocean.

Acknowledgements

We express our deep appreciation to the captain, crew and scientists on board the R/V *Mirai* MR12-E03 cruise for their assistance at sea and analyses of nutrients. We also thank Dr. A. Fujiwara (JAMSTEC) for his help with the information of the sea-ice distribution over our observation period. We are also grateful to Dr. M. Yamamoto-Kawai for her helpful discussion. This work is part of the Japanese initiative “Arctic Climate Change Research Project” within the GRENE (Green Network of Excellence) program. The data of hydrography, nutrients and sea-ice meltwater fraction used in this study were released from the Data Research System for Whole Cruise Information in JAMSTEC (Darwin, http://www.godac.jamstec.go.jp/darwin/e).

References

Aagaard, K., Coachman, L.K., Carmack, E., 1981. On the halocline of the Arctic Ocean. Deep-Sea Res. 28A (6), 529-545.

Aagaard, K., Carmack, E.C., 1989. The role of sea ice and other fresh water in the Arctic circulation. J. Geophys. Res. 94 (C10), 14485-14498.

Aguilar-Islas, A.M., Rember, R.D., Mordy, C.W., Wu, J., 2008. Sea ice-derived dissolved iron and its potential influence on the spring algal bloom in the Bering Sea. Geophys. Res. Lett. 35 (L24601), doi:10.1029/2008gl035736.

Aguilar-Islas, A.M., Rember, R., Nishino, S., Kikuchi, T., Itoh, M., 2013. Partitioning and lateral transport of iron to the Canada Basin. Polar Sci. 7 (2), 82-99.

Alonso-Saez, L., Waller, A.S., Mende, D.R., Bakker, K., Farnelid, H., Yager, P.L., Lovejoy, C., Tremblay, J.-É., Potvin, M., Heinrich, F., Estrada, M., Riemann, L., Bork, P., Pedros-Alio, C., Bertilsson, S., 2012. Role for urea in nitrification by polar marine Archaea. Proc. Natl. Acad. Sci. USA 109 (44), 17989-17994.

Anderson, L.G., Andersson, P.S., Björk, G., Peter Jones, E., Jutterström, S., Wåhlström, I., 2013. Source and formation of the upper halocline of the Arctic Ocean. J. Geophys. Res. Oceans 118 (1), 410-421.

Biller, D.V., Bruland, K.W., 2013. Sources and distributions of Mn, Fe, Co, Ni, Cu, Zn, and Cd relative to macronutrients along the central California coast during the spring and summer upwelling season. Mar. Chem. 155, 50-70.

Brown, Z.W., Casciotti, K.L., Pickart, R.S., Swift, J.H., Arrigo, K.R., 2015. Aspects of the marine nitrogen cycle of the Chukchi Sea shelf and Canada Basin. Deep-Sea Res. II 118, 73-87.

Bruland, K.W., 1980. Oceanographic distributions of cadmium, zinc, nickel, and copper in the North Pacific. Earth Planet. Sci. Lett. 47, 176-198.

Bruland, K.W., Donat, J.R., Hutchins, D.A., 1991. Interactive influences of bioactive trace metals on biological production in oceanic waters. Limnol. Oceanogr. 36 (8), 1555-1577.

Campbell, J.A., Yeats, P.A., 1982. The distribution of manganese, iron, nickel, copper and cadmium in the waters of Baffin Bay and Canadian Arctic Archipelago. Oceanol. Acta 5 (2), 161-168.

Chang, B.X., Devol, A.H., 2009. Seasonal and spatial patterns of sedimentary denitrification rates in the Chukchi sea. Deep-Sea Res. II 56 (17), 1339-1350.

Chester, R., Jickells, T., 2012. Marine geochemistry, third ed. Wiley-Blackwell, Oxford.

Chever, F., Rouxel, O.J., Croot, P.L., Ponzevera, E., Wuttig, K., Auro, M., 2015. Total dissolvable and dissolved iron isotopes in the water column of the Peru upwelling regime. Geochim. Cosmochim. Acta 162, 66-82.

Cid, A.P., Urushihara, S., Minami, T., Norisuye, K., Sohrin, Y., 2011. Stoichiometry among bioactive trace metals in seawater on the Bering Sea shelf. J. Oceanogr. 67 (6), 747-764.

Cid, A.P., Nakatsuka, S., Sohrin, Y., 2012. Stoichiometry among bioactive trace metals in the Chukchi and Beaufort Seas. J. Oceanogr. 68 (6), 985-1001.

Coachman, L.K., Aagaard, K., 1988. Transports through Bering Strait: Annual and interannual variability. J. Geophys. Res. 93 (C12), 15535-15539.

Codispoti, L.A., Flagg, C., Kelly, V., Swift, J.H., 2005. Hydrographic conditions during the 2002 SBI process experiments. Deep-Sea Res. II 52 (24-26), 3199-3226.

Connelly, T.L., Baer, S.E., Cooper, J.T., Bronk, D.A., Wawrik, B., 2014. Urea uptake and carbon fixation by marine pelagic bacteria and archaea during the Arctic summer and winter seasons. Appl. Environ. Microbiol. 80 (19), 6013-6022.

Cooper, L.W., Whitledge, T.E., Grebmeier, J.M., Weingartner, T., 1997. The nutrient, salinity, and stable oxygen isotope composition of Bering and Chukchi Seas waters in and near the Bering Strait. J. Geophys. Res. Oceans 102 (C6), 12563-12573.

Cullen, J.T., 2006. On the nonlinear relationship between dissolved cadmium and phosphate in the modern global ocean: Could chronic iron limitation of phytoplankton growth cause the kink? Limnol. Oceanogr. 51 (3), 1369-1380.

Deutsch, C., Weber, T., 2012. Nutrient ratios as a tracer and driver of ocean biogeochemistry. Ann. Rev. Mar. Sci. 4, 113-141.

Devol, A.H., 1978. Bacterial oxygen uptake kinetics as related to biological processes in oxygen deficient zones of the oceans. Deep-Sea Res. 25 (2), 137-146.

Dittmar, T., Kattner, G., 2003. The biogeochemistry of the river and shelf ecosystem of the Arctic Ocean: a review. Mar. Chem. 83 (3-4), 103-120.

Doxaran, D., Devred, E., Babin, M., 2015. A 50 % increase in the mass of terrestrial particles delivered by the Mackenzie River into the Beaufort Sea (Canadian Arctic Ocean) over the last 10 years. Biogeosciences, 12, 3551–3565.

Dupont, C.L., Buck, K.N., Palenik, B., Barbeau, K., 2010. Nickel utilization in phytoplankton assemblages from contrasting oceanic regimes. Deep-Sea Res. I 57 (4), 553-566.

Fujishima, Y., Ueda, K., Maruo, M., Nakayama, E., Tokutome, C., Hasegawa, H., Matsui, M., Sohrin, Y., 2001. Distribution of trace bioelements in the subarctic North Pacific Ocean and the Bering Sea (the R/V Hakuho Maru cruise KH-97-2). J. Oceanogr. 57, 261-273.

Griffin, C.G., Frey, K., Rogan, J., Holmes, R.M., 2011. Spatial and interannual variability of dissolved organic matter in the Kolyma River, East Siberia, observed using satellite imagery. J. Geophys. Res., 116, G03018, doi:10.1029/2010JG001634.

Gruber, N., Sarmiento, J.L., 1997. Global patterns of marine nitrogen fixation and denitrification. Glob. Biogeochemi. Cycles 11 (2), 235-266.

Hill, V., Cota, G., 2005. Spatial patterns of primary production on the shelf, slope and basin of the Western Arctic in 2002. Deep-Sea Res. II 52 (24-26), 3344-3354.

Hill, V., Cota, G., Stockwell, D., 2005. Spring and summer phytoplankton communities in the Chukchi and Eastern Beaufort Seas. Deep-Sea Res. II 52 (24-26), 3369-3385.

Hioki, N., Kuma, K., Morita, Y., Sasayama, R., Ooki, A., Kondo, Y., Obata, H., Nishioka, J., Yamashita, Y., Nishino, S., Kikuchi, T., Aoyama, M., 2014. Laterally spreading iron, humic-like dissolved organic matter and nutrients in cold, dense subsurface water of the Arctic Ocean. Sci. Rep. 4 (6775), doi:10.1038/srep06775.

Horner, T.J., Lee, R.B., Henderson, G.M., Rickaby, R.E.M., 2013. Nonspecific uptake and homeostasis drive the oceanic cadmium cycle. Proc. Natl. Acad. Sci. USA 110 (7), 2500-2505.

Johnson, K.S., Boyle, E.A., Bruland, K.W., Coale, K., Measures, C., Moffett, J., Aguilar-Islas, A., Barbeau, K., Bergquist, B.A., Bowie, A., Buck, K., Cai, Y., Chase, Z., Cullen, J., Doi, T., Elrod, V., Fitzwater, S., Gordon, M., King, A., Laan, P., Laglera-Baquer, L., Landing, W., Lohan, M., Mendez, J., Milne, A., Obata, H., Ossiander, L., Plant, J., Sarthou, G., Sedwick, P., Smith, G.J., Sohst, B., Tanner, S., van den Berg, S., Wu, J., 2007. Developing standards for dissolved iron in seawater. EOS 88 (11), 131-132.

Jones, E.P., Anderson, L.G., 1986. On the origin of the chemical properties of the Arctic Ocean halocline. J. Geophys. Res. 91 (C9), 10759-10767.

Kanna, N., Toyota, T., Nishioka, J., 2014. Iron and macro-nutrient concentrations in sea ice and their impact on the nutritional status of surface waters in the southern Okhotsk Sea. Prog. Oceanogr. 126, 44-57.

Kikuchi, T., 2012. R/V Mirai Cruise Report MR12-E03. In: Kikuchi, T., Nishino, S. (Eds.). JAMSTEC, Yokosuka, Japan, p. 199.

Kim, T., Obata, H., Kondo, Y., Ogawa, H., Gamo, T., 2015. Distribution and speciation of dissolved zinc in the western North Pacific and its adjacent seas. Mar. Chem. 173, 330-341.

Klunder, M.B., Bauch, D., Laan, P., de Baar, H.J.W., van Heuven, S., Ober, S., 2012a. Dissolved iron in the Arctic shelf seas and surface waters of the central Arctic Ocean: Impact of Arctic river water and ice-melt. J. Geophys. Res. 117, C01027,, doi:10.1029/2011JC007133.

Klunder, M.B., Laan, P., Middag, R., de Baar, H.J.W., Bakker, K., 2012b. Dissolved iron in the Arctic Ocean: Important role of hydrothermal sources, shelf input and scavenging removal. J. Geophys. Res. 117, C04014, doi:10.1029/2011JC007135.

Kondo, Y., Takeda, S., Furuya, K., 2012. Distinct trends in dissolved Fe speciation between shallow and deep waters in the Pacific Ocean. Mar. Chem. 134-135, 18-28.

Laglera, L.M., Battaglia, G., van den Berg, C.M.G., 2011. Effect of humic substances on the iron speciation in natural waters by CLE/CSV. Mar. Chem. 127 (1-4), 134-143.

Lambelet, M., Rehkämper, M., van de Flierdt, T., Xue, Z., Kreissig, K., Coles, B., Porcelli, D., Andersson, P., 2013. Isotopic analysis of Cd in the mixing zone of Siberian rivers with the Arctic Ocean—New constraints on marine Cd cycling and the isotope composition of riverine Cd. Earth Planet. Sci. Lett. 361, 64-73.

Lane, T.W., Morel, F.M.M., 2000. A biological function for cadmium in marine diatoms. Proc. Natl. Acad. Sci. USA 97 (9), 4627-4631.

Lohan, M.C., Bruland, K.W., 2008. Elevated Fe(II) and dissolved Fe in hypoxic shelf waters off Oregon and Washington: An enhanced source of iron to coastal upwelling regimes. Environ. Sci. Technol. 42 (17), 6462-6468.

Measures, C.I., 1999. The role of entrained sediments in sea ice in the distribution of aluminium and iron in the surface waters of the Arctic Ocean. Mar. Chem. 68, 59-70.

Middag, R., de Baar, H.J.W., Laan, P., Klunder, M.B., 2011. Fluvial and hydrothermal input of manganese into the Arctic Ocean. Geochimica et Cosmochimica Acta 75 (9), 2393-2408.

Millero, F.J., Sotolongo, S., Izaguirre, M., 1987. The oxidation kinetics of Fe(II) in seawater. Geochim. Cosmochim. Acta 51, 793-801.

Moore, C.M., Mills, M.M., Arrigo, K.R., Berman-Frank, I., Bopp, L., Boyd, P.W., Galbraith, E.D., Geider, R.J., Guieu, C., Jaccard, S.L., Jickells, T.D., La Roche, J., Lenton, T.M., Mahowald, N.M., Marañón, E., Marinov, I., Moore, J.K., Nakatsuka, T., Oschlies, A., Saito, M.A., Thingstad, T.F., Tsuda, A., Ulloa, O., 2013. Processes and patterns of oceanic nutrient limitation. Nature Geosci. 6 (9), 701-710.

Morgan, J.J., 2005. Kinetics of reaction between O2 and Mn(II) species in aqueous solutions. Geochim. Cosmochim. Acta 69 (1), 35-48.

Morison, J., Kwok, R., Peralta-Ferriz, C., Alkire, M., Rigor, I., Andersen, R., Steele, M., 2012. Changing Arctic Ocean freshwater pathways. Natute 481, 66-70.

Naidu, A.S., Blanchard, A., Kelley, J.J., Goering, J.J., Hameedi, M.J., Baskaran, M., 1997. Heavy metals in Chukchi Sea sediments as compared to selected circum-arctic shelves. Mar. Pollut. Bull. 35 (7-12), 260-269.

Nakayama, Y., Fujita, S., Kuma, K., Shimada, K., 2011. Iron and humic-type fluorescent dissolved organic matter in the Chukchi Sea and Canada Basin of the western Arctic Ocean. J. Geophys. Res. 116, C07031,, doi:10.1029/2010JC006779.

Nishimura, S., Kuma, K., Ishikawa, S., Omata, A., Saitoh, S.-i., 2012. Iron, nutrients, and humic-type fluorescent dissolved organic matter in the northern Bering Sea shelf, Bering Strait, and Chukchi Sea. J. Geophys. Res. 117, C02025, doi:10.1029/2011JC007355.

Nishino, S., Shimada, K., Itoh, M., 2005. Use of ammonium and other nitrogen tracers to investigate the spreading of shelf waters in the western Arctic halocline. J. Geophys. Res. 110 (C10005), doi:10.1029/2003JC002118.

Nishino, S., Itoh, M., Kawaguchi, Y., Kikuchi, T., Aoyama, M., 2011. Impact of an unusually large warm-core eddy on distributions of nutrients and phytoplankton in the southwestern Canada Basin during late summer/early fall 2010. Geophys. Res. Lett. 38, L16602, doi:16610.11029/12011GL047885.

Nishino, S., Kikuchi, T., Fujiwara, A., Hirawake, T., Aoyama, M., 2016. Water mass characteristics and their temporal changes in a biological hotspot in the southern Chukchi Sea. Biogeosciences 13 (8), 2563-2578.
Noble, A.E., Moran, D.M., Allen, A.E., Saito, M.A., 2013. Dissolved and particulate trace metal micronutrients under the McMurdo Sound seasonal sea ice: basal sea ice communities as a capacitor for iron. Front. Chem. 1, 25, doi:10.3389/fchem.2013.00025.
Obata, H., Karatani, H., Matsui, M., Nakayama, E., 1997. Fundamental studies for chemical speciation of iron in seawater with an improved analytical method. Mar. Chem. 56, 97-106.
Pakhomova, S.V., Hall, P.O.J., Kononets, M.Y., Rozanov, A.G., Tengberg, A., Vershinin, A.V., 2007. Fluxes of iron and manganese across the sediment–water interface under various redox conditions. Mar. Chem. 107 (3), 319-331.
Parekh, P., Follows, M.J., Boyle, E.A., 2005. Decoupling of iron and phosphate in the global ocean. Global Biogeochemical Cycles 19, GB2020, doi:2010.1029/2004GB002280.
Proshutinsky, A., Krishfield, R., Timmermans, M.-L., Toole, J., Carmack, E., McLaughlin, F., Williams, W.J., Zimmermann, S., Itoh, M., Shimada, K., 2009. Beaufort Gyre freshwater reservoir: State and variability from observations. J. Geophys. Res. 114, C00A10, doi:10.1029/2008JC005104.
Rachold, V., Eicken, H., Gordeev, V.V., Grigoriev, M.N., Hubberten, H.W., Lisitzin, A.P., Shevchenko, V.P., Schirrmeister, L., 2004. Modern terrigenous organic carbon input to the Arctic Ocean. In: The Organic Carbon Cycles in the Arctic Ocean, Ed: Stein, R., MacDonald, R.W., Springer, pp33-55.
Roshan, S., Wu, J., 2015. Water mass mixing: The dominant control on the zinc distribution in the North Atlantic Ocean. Glob. Biogeochem. Cycles 29 (7), 1060-1074.
Santana-Casiano, J.M., Gonzalez-Davila, M., Millero, F.J., 2005. Oxidation of nanomolar levels of Fe(II) with oxygen in natural waters. Environ. Sci. Technol. 39, 2073-2079.
Shimada, K., Ito, M., Nishino, S., McLaughlin, F., Carmack, E., Proshutinsky, A., 2005. Halocline structure in the Canada Basin of the Arctic Ocean. Geophys. Res. Lett. 32. L03605, doi:10.1029/2004GL021358.
Sohrin, Y., Urushihara, S., Nakatsuka, S., Kono, T., Higo, E., Minami, T., Norisuye, K., Umetani, S., 2008. Multielemental determination of GEOTRACES key trace metals in seawater by ICPMS after preconcentration using an ethylenediaminetriacetic acid chelating resin. Anal. Chem. 80, 6267-6273.
Springer, A.M., McRoy, C.P., 1993. The paradox of pelagic food webs in the northern Bering Sea—III. Patterns of primary production. Cont. Shelf Res. 13 (5-6), 575-599.
Stolpe, B., Hassellov, M., 2010. Nanofibrils and other colloidal biopolymers binding trace elements in coastal seawater: Significance for variations in element size distributions. Limnol. Oceanogr. 55 (1), 187-202.
Sunda, W.G., Huntsman, S.A., 1987. Microbial oxidation of manganese in a North Carolina estuary. Limnol. Oceanogr. 32 (3), 552-564.
Sunda, W.G., Huntsman, S.A., 1988. Effect of sunlight on redox cycles of manganese in the southwestern Sargasso Sea. Deep-Sea Res. A 35 (8), 1297-1317.
Sunda, W.G., Huntsman, S.A., 1990. Diel cycles in microbial manganese oxidation and manganese redox speciation in coastal waters of the Bahama Islands. Limnol. Oceanogr. 35 (2), 325-338.
Sunda, W.G., Huntsman, S.A., 2000. Effect of Zn, Mn and Fe on Cd accumulation in phytoplankton: Implications for oceanic Cd cycling. Limnol. Oceanogr. 45 (7), 1501-1516.
Swift, J.H., Jones, E.P., Aagaard, K., Carmack, E.C., Hingston, M., Macdonald, R.W., McLaughlin, F.A., Perkin, R.G., 1997. Waters of the Makarov and Canada basins. Deep-Sea Res. II 44 (8), 1503-1529.
Thuróczy, C.E., Gerringa, L.J.A., Klunder, M., Laan, P., Le Guitton, M., de Baar, H.J.W., 2011. Distinct trends in the speciation of iron between the shallow shelf seas and the deep basins of the Arctic Ocean. J. Geophys. Res. 116. C10009, doi:10.1029/2010JC006835.

Tovar-Sánchez, A., Duarte, C.M., Alonso, J.C., Lacorte, S., Tauler, R., Galbán-Malagón, C., 2010. Impacts of metals and nutrients released from melting multiyear Arctic sea ice. J. Geophys. Res. 115, C07003, doi:10.1029/2009JC005685.

Trefry, J.H., Trocine, R.P., Cooper, L.W., Dunton, K.H., 2014. Trace metals and organic carbon in sediments of the northeastern Chukchi Sea. Deep-Sea Res. II 102, 18-31.

Twining, B.S., Baines, S.B., 2013. The trace metal composition of marine phytoplankton. Ann. Rev. Mar. Sci. 5, 191-215.

von Langen, P.J., Johnson, K.S., Coale, K.H., Elrod, V., 1997. Oxidation kinetics of manganese(II) in seawater at nanomolar concentrations. Geochim. Cosmochim. Acta 61 (23), 4945-4954.

Wang, D., Henrichs, S.M., Guo, L., 2006. Distributions of nutrients, dissolved organic carbon and carbohydrates in the western Arctic Ocean. Cont. Shelf Res. 26 (14), 1654-1667.

Watanabe, E., Onodera, J., Harada, N., Aita, M.N., Ishida, A., Kishi, M.J., 2015. Wind-driven interannual variability of sea ice algal production in the western Arctic Chukchi Borderland. Biogeosciences 12 (20), 6147-6168.

Wickland, K.P., Aiken, G.R., Butler, K., Dornblaser, M.M., Spencer, R.G.M., Striegl, R.G., 2012. Biodegradability of dissolved organic carbon in the Yukon River and its tributaries: Seasonality and importance of inorganic nitrogen. Glob. Biogeochem. Cycles 26, GB0E03, doi:10.1029/2012GB004342.

Wolfe-Simon, F., Grzebyk, D., Schofield, O., Falkowski, P.G., 2005. The role and evolution of superoxide dismutases in algae. J. Phycol. 41, 453-465.

Wood, K.R., Bond, N.A., Danielson, S.L., Overland, J.E., Salo, S.A., Stabeno, P.J., Whitefield, J., 2015. A decade of environmental change in the Pacific Arctic region. Prog. Oceanogr. 136, 12-31.

Yamada, Y., Fukuda, H., Uchimiya, M., Motegi, C., Nishino, S., Kikuchi, T., Nagata, T., 2015. Localized accumulation and a shelf-basin gradient of particles in the Chukchi Sea and Canada Basin, western Arctic. J. Geophys. Res. Oceans 120 (7), 4638-4653.

Yamamoto-Kawai, M., Carmack, E., McLaughlin, F., 2006. Nitrogen balance and Arctic throughflow. Nature 443, 43.

Yamamoto-Kawai, M., McLaughlin, F.A., Carmack, E.C., Nishino, S., Shimada, K., 2008. Freshwater budget of the Canada Basin, Arctic Ocean, from salinity, δ 18O, and nutrients. J. Geophys. Res. 113. C01007, doi:10.1029/2006JC003858.

Yamamoto-Kawai, M., McLaughlin, F.A., Carmack, E.C., Nishino, S., Shimada, K., Kurita, N., 2009. Surface freshening of the Canada Basin, 2003–2007: River runoff versus sea ice meltwater. J. Geophys. Res. 114, C00A05, doi:10.1029/2008JC005000.

Yeats, P.A., 1988. Manganese, nickel, zinc and cadmium distributions at the Fram 3 and Cesar ice camps in the Arctic Ocean. Oceanol. Acta 11 (4), 383-388.

Yeats, P.A., Westerlund, S., 1991. Trace metal distributions at the Arctic Ocean ice island. Mar. Chem. 33, 261-277.

Table 1. Values for SAFe D2 and GEOTRACES intercalibration 2009 GD samples for Mn, Fe, Ni, Zn and Cd in this study.

Sample		Mn	Fe	Ni	Zn	Cd
D2	This study	0.39 ± 0.07 (n=3)	0.81 ± 0.11 (n=3)	8.47 (n=1)	7.53 (n=2)	1.10 ± 0.10 (n=3)
	Consensus value	0.35 ± 0.05	0.93 ± 0.02	8.63 ± 0.25	7.43 ± 0.25	0.99 ± 0.02
GD	This study	0.25 (n=2)	1.14 (n=2)	4.07 (n=2)	2.25 (n=1)	0.30 (n=2)
	Consensus value	0.21 ± 0.03	1.00 ± 0.10	4.00 ± 0.10	1.71 ± 0.12	0.271 ± 0.001

Table 2.

Concentrations of dissolved trace metals (D-Mn, D-Fe, D-Ni, D-Zn and D-Cd), total dissolvable trace metals (TD-Mn, TD-Fe, TD-Ni, TD-Zn and TD-Cd) and chlorophyll *a* (Chl *a*) in the western Arctic Ocean.

Station	Depth (m)	[D-Mn] (nM)	[D-Fe] (nM)	[D-Ni] (nM)	[D-Zn] (nM)	[D-Cd] (nM)	[TD-Mn] (nM)	[TD-Fe] (nM)	[TD-Ni] (nM)	[TD-Zn] (nM)	[TD-Cd] (nM)	Chl *a* (μg/L)
D1	5	8.31	1.48	5.52	2.75	0.34	12.8	8.35	5.66	3.19	0.38	
(72.00,02' N,	10	8.91	1.11	5.63	2.50	0.40	17.6	9.67	5.65	3.49	0.45	0.43
159.99,72' W)	20	34.9	6.00	6.52	3.69	0.65	44.1	1173	6.97	6.57	0.70	0.32
D2	5	14.2	1.82	6.35	2.62	0.25	24.0	20.5	5.40	4.01	0.35	
(72.49,98' N,	10	11.3	1.64	5.12	1.16	0.11	24.5	21.2	5.54	1.58	0.36	0.41
158.79,88' W)	20	8.61	1.19	6.62	2.62	0.34	10.8	7.26	5.88*	2.17*	0.46	0.42
	30	5.14	1.78	7.84	2.57	0.61	18.1	17.5	6.63*	2.64	0.75	
	40	33.0	5.25	8.12	4.82	0.75	39.2	240	6.84*	4.79*	0.92	0.24
	46	81.4	8.26	8.76	6.18	0.86	115	3276	11.46	13.8	1.12	
D3	5	15.0	2.65	5.94	1.62	0.38	37.8	36.0	7.85	2.56	0.41	
(72.86,53' N,	10	13.1	1.17	5.47	1.35	0.22	36.6	30.6	7.21	2.24	0.39	0.50
157.96,47' W)	30	6.09	1.37	5.96	2.19	0.54	22.9	65.8	N.D.	2.83	0.54	0.48
	50	7.38	2.12	6.77	2.77	0.76	25.8	74.2	7.16	3.56	0.65*	0.05
	75	12.0	3.72	7.57	4.69	0.92	23.4	57.9	7.59	5.62	0.99	0.03
	100	42.6	5.09	7.42	4.58	0.99	67.6	254	8.59	6.54	0.98*	0.06
	125	57.3	5.39	6.69	4.61	0.79	83.5	179	7.61	6.23	1.31	0.05
	150	13.2	3.12	5.26	3.12	0.51	33.7	79.1	5.29	4.02	0.47*	0.01
	200	1.08	1.99	3.90	2.36	0.34	6.00	24.1	4.12	4.42	0.40	0.00
	300	0.69	1.33	3.21	2.14	0.28	8.45	56.3	3.54	3.72	0.38	
	400	0.53	0.95	3.00	1.69	0.24	2.37	7.84	3.07	1.77	0.23*	
	500	0.42	1.52	3.37	1.76	0.24	2.98	13.5	3.18*	2.90	0.31	

N.D. = not determined.

* Recovery of trace metals from the unfiltered sample may not be sufficient.

Table 2. continued.

Station	Depth (m)	[D-Mn] (nM)	[D-Fe] (nM)	[D-Ni] (nM)	[D-Zn] (nM)	[D-Cd] (nM)	[TD-Mn] (nM)	[TD-Fe] (nM)	[TD-Ni] (nM)	[TD-Zn] (nM)	[TD-Cd] (nM)	Chl *a* (μg/L)
D4	5	8.36	1.66	6.62	3.12	0.20	9.48	4.38	6.59*	3.46	0.18*	0.09
(73.49.22' N	10	7.65	1.04	6.34	1.52	0.12	10.21	4.11	6.89	4.83	0.21	0.09
156.41.15' W)	25	5.96	1.41	7.55	1.37	0.23	6.57	2.11	6.66*	1.61	0.22*	0.08
	50	4.90	1.78	6.17	0.62	0.20	5.49	N.D.	6.81	1.43	0.25	0.15
	75	2.83	N.D.	8.86	2.18	0.29	2.86	2.25	6.15*	1.70*	0.37	0.10
	100	1.52	2.71	7.85	3.16	0.51	3.61	7.06	7.73*	3.88	0.79	0.02
	150	13.61	2.84	7.76	4.40	0.60	22.3	18.2	7.62*	4.03*	0.63	0.00
	200	17.89	3.35	7.64	5.91	0.68	32.4	56.6	8.36	6.47	0.83	0.01
	250	1.02	1.53	4.42	3.11	0.31	5.10	18.6	4.54	3.84	0.65	
	300	0.74	1.36	3.37	2.32	0.22	4.00	12.9	4.16	4.45	0.30	
	400	0.52	1.17	3.78	2.06	0.18	2.81	5.68	3.50*	2.09	0.20	
	500	0.56	5.00	4.17	2.37	0.12	2.68	5.38	3.49	2.65	0.25	
D5	5	8.21	N.D.	N.D.	N.D.	0.25	9.70	3.13	6.83	3.53	0.34	
(74.49.87' N,	10	7.71	N.D.	6.58	N.D.	0.23	10.3	2.91	7.20	1.84	0.34	0.06
154.00.40' W)	25	5.48	N.D.	5.91	1.05	0.29	7.59	2.72	7.30	2.70	0.30	
	50	3.86	N.D.	5.91	0.76	0.25	4.82	1.47	7.25	0.71*	0.40	0.09
	75	1.82	1.52	5.83	1.82	0.40	3.21	1.80	7.03	2.81	0.58	0.15
	100	1.10	1.40	5.33	3.02	0.48	3.51	2.25	7.26	4.59	0.66	0.22
	150	2.04	1.81	6.65	3.81	0.65	5.89	5.38	7.94	4.52	0.71	
	200	1.99	1.20	6.79	4.83	0.69	6.26	5.87	8.66	5.44	0.69	
	250	0.89	1.34	4.65	3.42	0.48	4.21	6.80	5.80	3.79	0.57	
	300	0.67	2.34	3.41	N.D.	0.37	2.99	4.99	4.12	7.55	0.33*	
	400	0.44	1.18	2.84	2.08	0.26	2.45	7.50	3.71	2.73	0.28	
	500	0.34	0.78	2.72	1.62	0.26	2.28	5.54	3.73	2.20	0.30	

N.D. = not determined.

* Recovery of trace metals from the unfiltered sample may not be sufficient.